THEMED ISSUE: Tectonics at the Micro- to Macroscale: Contributions in Honor of the University of Michigan Structure-Tectonics Research Group of Ben van der Pluijm and Rob Van der Voo

THE GEOLOGICAL SOCIETY OF AMERICA®

Neoproterozoic to early Paleozoic tectonic evolution of the Zavkhan terrane of Mongolia: Implications for continental growth in the Central Asian orogenic belt

Uyanga Bold[1], James L. Crowley[2], Emily F. Smith[3], Oyungerel Sambuu[4], and Francis A. Macdonald[1]

[1]DEPARTMENT OF EARTH AND PLANETARY SCIENCE, HARVARD UNIVERSITY, 20 OXFORD ST., CAMBRIDGE, MASSACHUSETTS 02138, USA
[2]DEPARTMENT OF GEOSCIENCES, BOISE STATE UNIVERSITY, 1910 UNIVERSITY DRIVE, BOISE, IDAHO 83725, USA
[3]DEPARTMENT OF PALEOBIOLOGY, SMITHSONIAN INSTITUTION, PO BOX 37012, MRC 121, WASHINGTON, D.C. 20013, USA
[4]SCHOOL OF GEOLOGY AND MINING ENGINEERING, MONGOLIAN UNIVERSITY OF SCIENCE AND TECHNOLOGY, 8TH KHOROO, BAGA TOIRUU 34, SUKHBAATAR DISTRICT, ULAANBAATAR 14191, MONGOLIA

ABSTRACT

The Zavkhan terrane is a Proterozoic cratonic fragments in southwestern Mongolia that forms the core of the Central Asian orogenic belt. We provide new geologic and U-Pb zircon geochronologic constraints on the Neoproterozoic and early Paleozoic tectonic evolution of the terrane. Orthogneisses dated as ca. 1967 and ca. 839 Ma form the basement and are intruded and overlain by ca. 811–787 Ma arc-volcanic and volcaniclastic rocks that lack a gneissic fabric, suggestive of a mid-Neoproterozoic metamorphic event. Rifting and formation of the Zavkhan ribbon continent occurred from ca. 770–717 Ma and was followed by passive margin sedimentation between 717 and 580 Ma. During the latest Ediacaran to Cambrian, the southern margin of the Zavkhan terrane was reactivated with the obduction of the Lake terrane, slab break-off and reversal, and ca. 509–507 Ma magmatism. Metamorphosed Proterozoic and Cambrian units are cut by undeformed ca. 496 Ma gabbro, providing a tight constraint on the age of Cambrian metamorphism. Late Ordovician to Silurian rifting is marked by bimodal magmatism and deposition in narrow fault-bound basins. Our data indicate that the Zavkhan terrane traveled alone in the Neoproterozoic, collided with the Lake terrane in the late Ediacaran to Cambrian, and accreted an unknown crustal block during Cambrian Epoch 2–Epoch 3 that rifted away in the Ordovician. We suggest the majority of continental growth in Mongolia occurred through the trapping and oroclinal bending of ribbon continents rather than long-lived accretion on the margin of a major craton.

LITHOSPHERE GSA Data Repository Item 2016344 doi:10.1130/L549.1

INTRODUCTION

The Central Asian orogenic belt (CAOB), also known as the Altaids, is located between the East European, Siberian, North China, and Tarim cratons and is considered the largest area of Phanerozoic continental crustal growth (Fig. 1A; e.g., Windley et al., 2007). Tectonic activity in the CAOB is commonly thought to have started ca. 1020 Ma (Khain et al., 2002) with the opening of the paleo-Asian Ocean (Dobretsov et al., 2003) and to have continued until its closure in the latest Permian (Xiao et al., 2003) or Jurassic (Van der Voo et al., 2015). The immense area and timescale of the CAOB point to its formation through multiple orogenic cycles; however, due to the lack of detailed geologic mapping and outdated geochronologic techniques, the nature and precise timing of these tectonic events have not been clearly delineated. In particular, it is unclear when and over what extent the CAOB was affected by accretionary or collisional processes (e.g., Schulmann and Paterson, 2011). Moreover, due to a dearth of robust U-Pb single zircon ages and paleomagnetic poles, the origin and travels of Proterozoic and early Paleozoic cratonic fragments in the CAOB remain poorly constrained. Precise geochronology, petrology, and paleomagnetic data integrated into new geologic mapping is needed to provide the necessary geologic context to create the next generation of models for continental growth and to assess when, where, and how the CAOB formed.

Mongolia is located in the heart of the CAOB (Fig. 1A) and its southwestern and northeastern regions constitute the Proterozoic cratonic fragments that are stitched together by Paleozoic arcs and accretionary zones (Fig. 1B; e.g., Dobretsov et al., 2003; Khain et al., 2003; Kröner et al., 2010; Lehmann et al., 2010; Wilhem et al., 2012; Windley et al., 2007; Yakubchuk, 2004). Previous studies have assumed a shared Proterozoic through Paleozoic geologic evolution between many of the Mongolian cratonic fragments (Kröner et al., 2011; Lehmann et al., 2010; Levashova et al., 2010; Wilhem et al., 2012; Windley et al., 2007). Although this assumption may be correct for some of the terranes, it has not been the direct result of detailed geologic observations or geochronologic constraints; there are no specific data that unequivocally support this model. Additional geochronologic data have been reported from several of the cratonic terranes (e.g., Kozakov et al., 2012b; Kuzmichev et al., 2005; Salnikova et al., 2001; Yarmolyuk et al., 2008), but they have not been integrated with geologic mapping and stratigraphy.

In this study, we present new geochronologic data and geologic mapping from the Zavkhan terrane. We then integrate these data with existing data from adjacent terranes to develop a new model for the tectonic

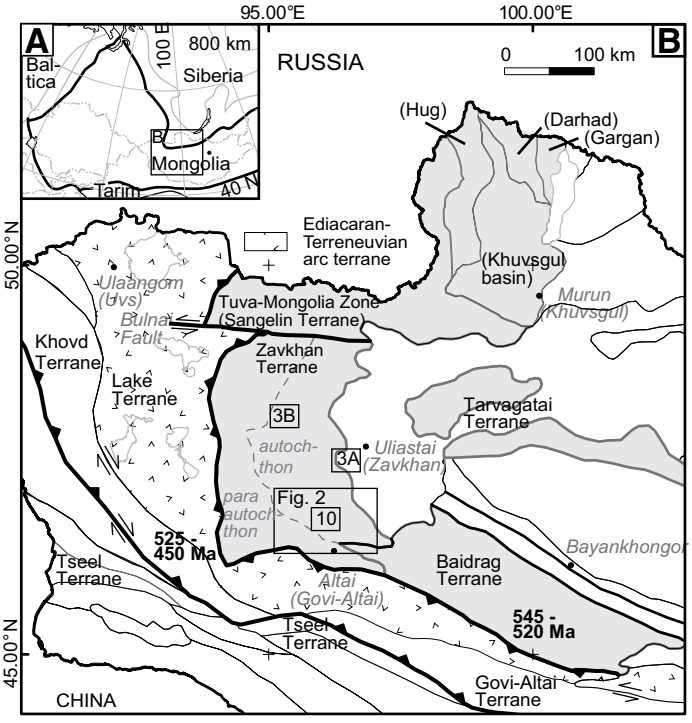

Figure 1. Location map of the study area. (A) Extent of Central Asian orogenic belt, illustrated after Şengör and Natal'in (1996) and Bucholz et al. (2014). (B) Terrane map of western Mongolia, modified from Badarch et al. (2002). Proterozoic cratonic fragments described in western Mongolia are shaded in light gray and Ediacaran-Terreneuvian arc terrane, the Lake terrane, is highlighted. The Tuva-Mongolia terranes borders the Zavkhan terrane to the north and it is composed of the Sangelin, Hug, Darhad, and Gargan terranes and Khuvsgul terranes (Badarch et al., 2002). Major tectonic structures near the Zavkhan terrane are highlighted along with estimated ages.

evolution of southwestern Mongolia, and discuss implications for continental growth in the CAOB.

Previous Models for the Proterozoic and early Paleozoic tectonic evolution of southwestern Mongolia

In Mongolia, the Paleozoic CAOB outlines Proterozoic terranes with crystalline basement (Fig. 1B). Through most of the twentieth century, the cratonic fragments of Mongolia were divided between the Tuva-Mongolia terranes (also referred to as the Tuva-Mongolia zone or massif) and central Mongolia (Ilyin, 1990); this served as the foundation for future geologic interpretation. By the turn of the century, the joint Mongolian and Russian 1:200,000 scale regional mapping projects provided additional relative age constraints on lithostratigraphic units. These data were central to the Kipchak-Tuva-Mongol magmatic arc model of Şengör et al. (1993). In this peri-Siberian arc model, continental growth occurred predominantly around a single Cambrian arc that formed on the margins of Siberia and Baltica, which was oroclinally bent and imbricated during the late Paleozoic (Şengör et al., 1993). With little attention to the Precambrian geology, Şengör et al. (1993) assumed that the Mongolian terranes were part of a peri-Siberian arc, floored by Siberian basement. Moreover, with little paleomagnetic evidence, Şengör et al. (1993) kept Mongolia close to Siberia throughout the Paleozoic, as have many others (e.g., Wilhem et al., 2012). Paleozoic fauna are commonly cited in referring to Mongolian terranes as peri-Siberian (e.g., Cocks and Torsvik, 2007) based on the similarity in trilobite assemblages found in Cambrian sedimentary rocks of some of the terranes north and west of the Zavkhan terrane with those endemic to Siberia (Astashkin et al., 1995), along with the Silurian *Tuvaella* brachiopod fauna, which is restricted to terranes in the CAOB but not found on the Siberian craton (Wang et al., 2011). Thus, direct paleontological ties between the Zavkhan terrane and the Siberian craton are equivocal and limited to the early Paleozoic between Mongolia and other peri-Siberian terranes and not directly to the Siberian craton.

Using a different approach, Mossakovsky et al. (1994) compared geologic data from Proterozoic regions of Mongolia, which they called the microcontinents of the southern CAOB, with data from North China, Tarim, Tien Shan, Ulutau, and Amur. Based on available stratigraphic sections of the Neoproterozoic and Cambrian terrigenous carbonate cover sequences of the Khuvsgul and Zavkhan terranes, Mossakovsky et al. (1994) suggested that the Mongolian cratonic terranes originated from eastern Gondwana and collided with Siberia during the Paleozoic. Building on this exotic collisional model with additional Paleozoic tectonostratigraphic, geochronologic, and Hf and Nd isotope data, Kröner et al. (2010) invoked repeated magmatic reworking of both proximal and distal passive margins of a composite peri-Gondwanan terrane (Kröner et al., 2014) prior to a final Permian collision with Siberia, Tarim, and North China. A northeast Gondwanan origin of the Mongolian terranes was also suggested by detrital zircon provenance data (Rojas-Agramonte et al., 2011); however, this study lumped samples from many regions within Mongolia, and the samples were mostly Paleozoic, yet were compared with mostly Precambrian samples from Tarim, North China, northeast Gondwana, and Siberia. Here we refer to these models that evoke a tectonic evolution of the Mongolian terranes independent of Siberia as exotic collisional models.

Badarch et al. (2002) used an approach in which they employed terrane analysis (Jones, 1983) to divide Mongolia into 44 cratonic, metamorphic, and passive continental margin terranes, and proposed an accretionary growth model on the Siberian margin with pulses of events in the Neoproterozoic, Cambrian-Ordovician, Devonian, Permian, and Triassic. This Siberian accretionary growth model (Windley et al., 2007) shares elements of both the peri-Siberian arc model and the exotic collisional model with the main-Mongolian lineament separating peri-Siberian and peri-Gondwanan terranes.

Sparse paleomagnetic data have been used variously to argue either for or against a Siberian origin for the Mongolian terranes. Levashova et al. (2010) used a paleomagnetic pole on the ca. 800 Ma old Zavkhan Formation volcanics (described therein as the Baydrag microcontinent) to argue for an origin from either India, South China, Tarim, or Australia. In addition, paleomagnetic data from Terreneuvian strata of the Zavkhan terrane suggested that it was far north from the equatorial Siberian craton at that time (Evans et al., 1996). However, another paleomagnetic study from the Neoproterozoic and Cambrian strata on the Zavkhan terrane suggested that these rocks formed adjacent to Siberia (Kravchinsky et al., 2001). These inconsistencies in the Neoproterozoic and Paleozoic paleolatitude of the Zavkhan terrane highlight the need for additional paleomagnetic data and a new synthesis of existing data (Kilian et al., 2016).

In summary, there are currently three broad classes of models for the Neoproterozoic to Paleozoic tectonic evolution of Mongolia: (1) a peri-Siberian arc model (e.g., Cocks and Torsvik, 2007; Şengör et al., 1993; Tomurtogoo, 2005; Wilhem et al., 2012), (2) a collisional model of exotic terranes (e.g., Kröner et al., 2014; Kröner et al., 2010; Mossakovsky et al., 1994), and (3) a Siberian accretionary growth model (Badarch et al., 2002; Windley et al., 2007). A key distinction of these models is that both the peri-Siberian arc model and the Siberian accretionary model predict that the Zavkhan terrane has Siberian basement and had a Paleozoic tectonic history similar to that of the southern margin of Siberia. In contrast, the

exotic collisional model predicts that the Proterozoic and Paleozoic geologic history of Mongolia should be distinct from that of Siberia.

Tectonic and Geologic setting of the Zavkhan terrane

The Zavkhan terrane is divided into two regions, an autochthonous region to the northeast and a parautochthonous region to the southwest (Figs. 1 and 2). The parautochthonous region was called the Urgamal subzone by Badarch et al. (2002) and the Altai allochthon by Bucholz et al. (2014) and Bold et al. (2016) due to prevalence of highly metamorphosed rock assemblage, the lack of the late Neoproterozoic to Terreneuvian overlap sequence that is characteristic of the Zavkhan terrane, and uncertainty of the age of basement. The parautochthon borders the Lake terrane (Ediacaran-Cambrian arc terrane, formerly known as the Lake zone) to the west, southwest, and south, and the autochthon borders the Baidrag terrane to the east, Tarvagatay terrane to the northeast, and Tuva-Mongolia terranes (particularly the Sangelin terrane) to the north, separated by the Bulnai fault (Fig. 1B; Rizza et al., 2015).

The Zavkhan terrane has been described as a cratonic terrane (Badarch et al., 2002) or a microcontinent (e.g., Lehmann et al., 2010; Wilhem et al., 2012) that hosts a gneissic basement as old as 1868 ± 3 Ma (Burashnikov, 1990); however, this date is a U/Pb thermal ionization mass spectrometry age on multigrain bulk zircon fractions with metamorphic rims and consequently likely incorporated zircon domains of different ages. Several attempts have been made to better constrain the age of the Zavkhan terrane basement. Zircon rims from a potassic leucosome within a migmatitic gneiss were dated from the Khavchig complex at 840 ± 9 Ma (sensitive high-resolution ion microprobe, SHRIMP, U-Pb zircon) with inherited zircon cores from 2445 to 1440 Ma (Zhao et al., 2006). In Zavkhanmandal soum (a local administrative division within the Zavkhan province), an additional granite gneiss was dated as 856 ± 2 Ma (multigrain bulk zircon fractions) (Kozakov et al., 2012b), suggesting there were several stages of magmatism and metamorphism in the region or a long-lasting migmatization event.

The parautochthonous region of the Zavkhan terrane is composed of amphibolite to granulite facies paragneisses and orthogneisses and greenschist facies metasedimentary and volcanic sequences (Figs. 2–4). The oldest unit of the parautochthon is the Khavchig complex (Togtokh et al., 1995), which consists of biotite, biotite amphibolite, and garnet gneiss with rare beds of quartzite and marble. It is overlain by the Yesonbulag Formation, which is composed of gneiss, amphibolite, and marble and intruded by gabbro, gabbro-diorite, and diorite of the Dund orthocomplex (Ruzhentsev and Burashnikov, 1996). Togtokh et al. (1995) distinguished metasedimentary units of the Yargait and Shandiinnuruu Formations above the Dund orthocomplex that are characterized by interbeds of metasediments, rhyolite, and dolerite, which are unconformably overlain by the Zavkhan Formation.

In the northwestern part of the Zavkhan terrane, the Zavkhan Formation unconformably overlies the Tsagaankhairkhan Formation, which is a carbonate sequence dominated by stromatolitic dolomite. Unfortunately, this unit is only exposed in western Khukh Davaa (Fig. 2) and has no apparent stratigraphic relationships with other units, and so its age relative to other pre-Zavkhan Formation units remains poorly constrained. The overlying Zavkhan Formation can be divided into two subunits. The lower Zavkhan Formation is dominated by boulder clast conglomerate, whereas rhyolite and minor mafic flows prevail in the upper portion. The age of the volcanism of the Zavkhan Formation is constrained by chemical abrasion-isotope dilution-thermal ionization mass spectrometry (CA-ID-TIMS) U-Pb dates on zircon that range from 802.11 ± 0.45–787.45 ± 0.47 Ma (Bold et al., 2016). The stratigraphy above the Zavkhan Formation was revised by Macdonald et al. (2009), Bold et al. (2013), and Smith et al. (2016) in detail following terrane-wide, member-level mapping. According to the revised stratigraphic nomenclature, the Khasagt Formation unconformably overlies volcanics of the Zavkhan Formation, which in turn is unconformably overlain by the Tsagaan-Olom Group (Bold et al., 2016).

The Khasagt Formation is composed of siltstone, sandstone, and conglomerate and has large lateral thickness changes. It is best exposed and thickest in the Khasagt Khairkhan Range, thinning toward the Khukh Davaa region, and is absent in the north of the Zavkhan terrane. These thickness changes represent both facies change, fault-controlled deposition in a narrow graben, and erosion beneath 717–660 Ma Sturtian glacial deposits of the overlying Maikhan-Uul Formation(Macdonald et al., 2010; Rooney et al., 2015), which forms the base of the Tsagaan-Olom Group. The Maikhan-Uul Formation is sharply overlain by carbonate strata of the Taishir Formation, which in turn overlain by ca. 635 Ma Marinoan glacial deposits of the Khongor Formation (Macdonald et al., 2009). Early Ediacaran carbonates of the overlying Ol and Shuurgat Formations are >500 m thick; the top of the Tsagaan-Olom Group is defined by a karstic unconformity (Bold et al., 2013). Overlying this unconformity are late Ediacaran phosphorite and carbonate strata of the Zuun-Arts Formation and mixed carbonates and siliciclastic strata of the Terreneuvian Bayangol, Salaagol, and Khairkhan Formations (Fig. 3), which record deposition in a foreland basin (Macdonald et al., 2009; Smith et al., 2016 .

In the Zavkhan terrane, the Terreneuvian Khairkhan Formation is overlain by Cambrian to Ordovician chert and cobble conglomerate units, and the Late Ordovician to Silurian Teel Formation (Kilian et al., 2016), which is composed of bimodal series of rhyolite and basalt with interbeds of conglomerate, sandstone, and siltstone (Togtokh et al., 1995). Regionally, red beds of the Teel Formation have been mapped erroneously as the Tsagaanshoroot Formation (Togtokh et al., 1995), which is composed of interbedded limestone, conglomerate, sandstone, siltstone, and rare beds of basalt in the parautochthonous region that preserves the Middle Devonian brachiopod *Wilsonella sp.* (Pojeta, 1986) and the progymnosperm *Aneruophyton sp.* (Petrosyan, 1967). The youngest sedimentary rocks in the region are in the Jurassic sedimentary sequence of the Jargalant Formation, which is exposed on the parautochthonous basement, in the southern opening of the Khoid and Dund Sharga Gorges of the Sharga soum of the Govi-Altai province (Fig. 2).

Paleozoic felsic magmatism is abundant in the Zavkhan terrane, but previously no plutons or volcanic rocks had been dated with the U-Pb zircon method. Based on map relationships, these intrusions have been correlated with the Paleozoic Numrug and Tonkhil complexes, which were considered to be Pennsylvanian and Permian, respectively (Togtokh et al., 1995).. Both of these Paleozoic granites are alkaline but the Tonkhil complex is characterized by coarse crystalline syenite porphyry. In the following we demonstrate that the Numrug complex is earliest Silurian in age; the age of the Permian Tonkhil complex is refined in Kilian et al. (2016).

METHODS

Sampling

From 2011 to 2015, in the course of geological mapping (Fig. 2), the main lithostratigraphic units (Fig. 5) were sampled for U-Pb zircon geochronology. In addition, in the Zavkhanmandal (U1520, Fig. 3B) and Aldarkhaan soums (U1519, Fig. 3A) of the northern Zavkhan province, granite gneisses of the Buduun Formation (Samozvantsen et al., 1981) were sampled to better constrain the age of the basement of the Zavkhan terrane. Petrographic thin sections were prepared at Harvard University (Cambridge, Massachusetts).

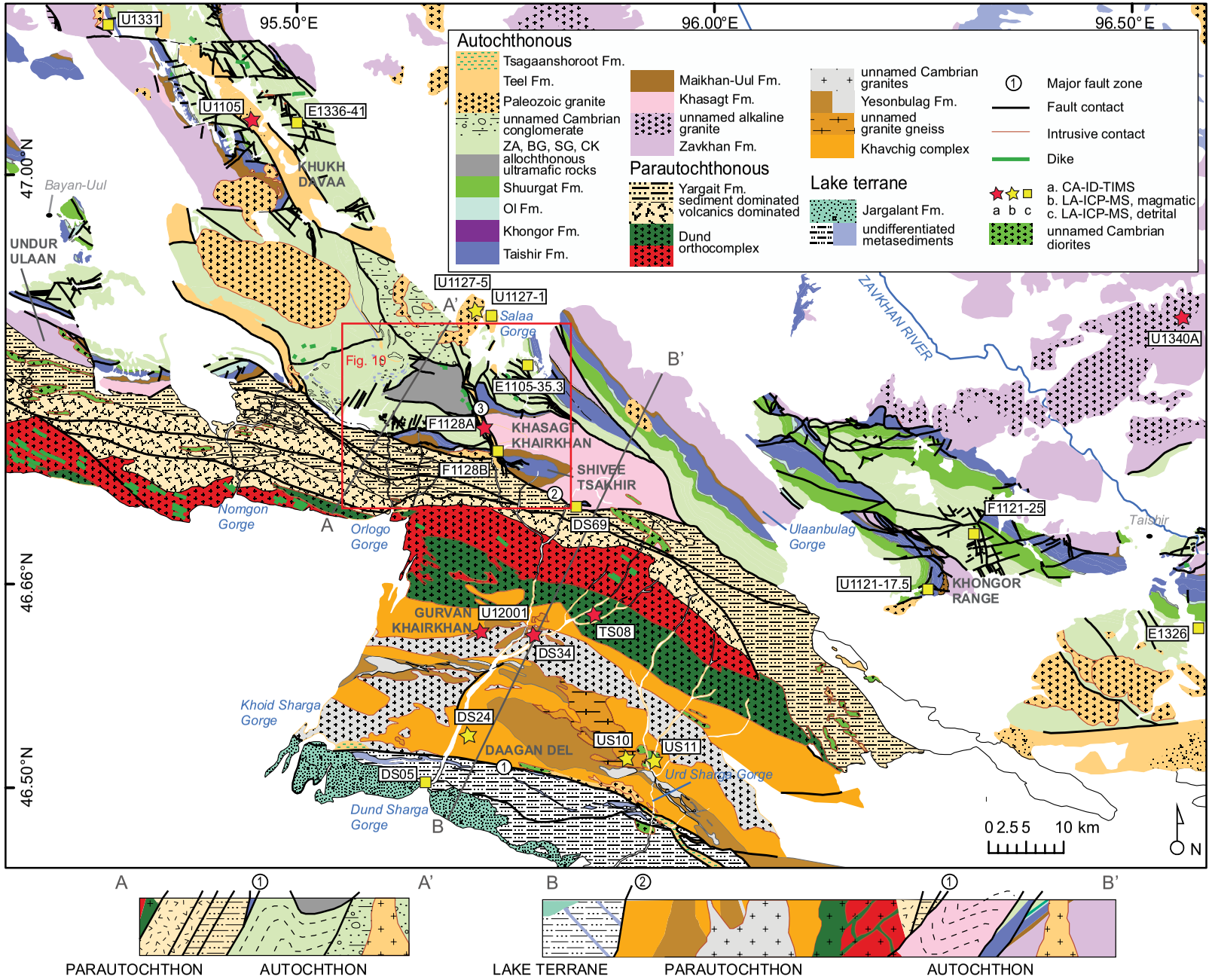

Figure 2. Geologic map of the Zavkhan terrane as mapped by three of us (Macdonald, Bold, and Smith). Mapping of parautochthonous region is adapted from Togtokh et al. (1995). Main fault zones are numbered from 1 to 4. Dated samples are labeled except U1519 and U1520 (Yarmolyuk et al., 2008); see Figure 3. Geochronologic results of samples U1105 and U1127–5 are described in Kilian et al. (2016). Abbreviations: LA-ICP-MS—laser ablation–inductively coupled plasma–mass spectrometry; CA-ID-TIMS—chemical abrasion–isotope dilution–thermal ionization mass spectrometry; Fm.—formation; ZA—Zuun-Arts Formation; BG—Bayangol Formation; SG—Salaagol Formation; CK—Khairkhan Formation.

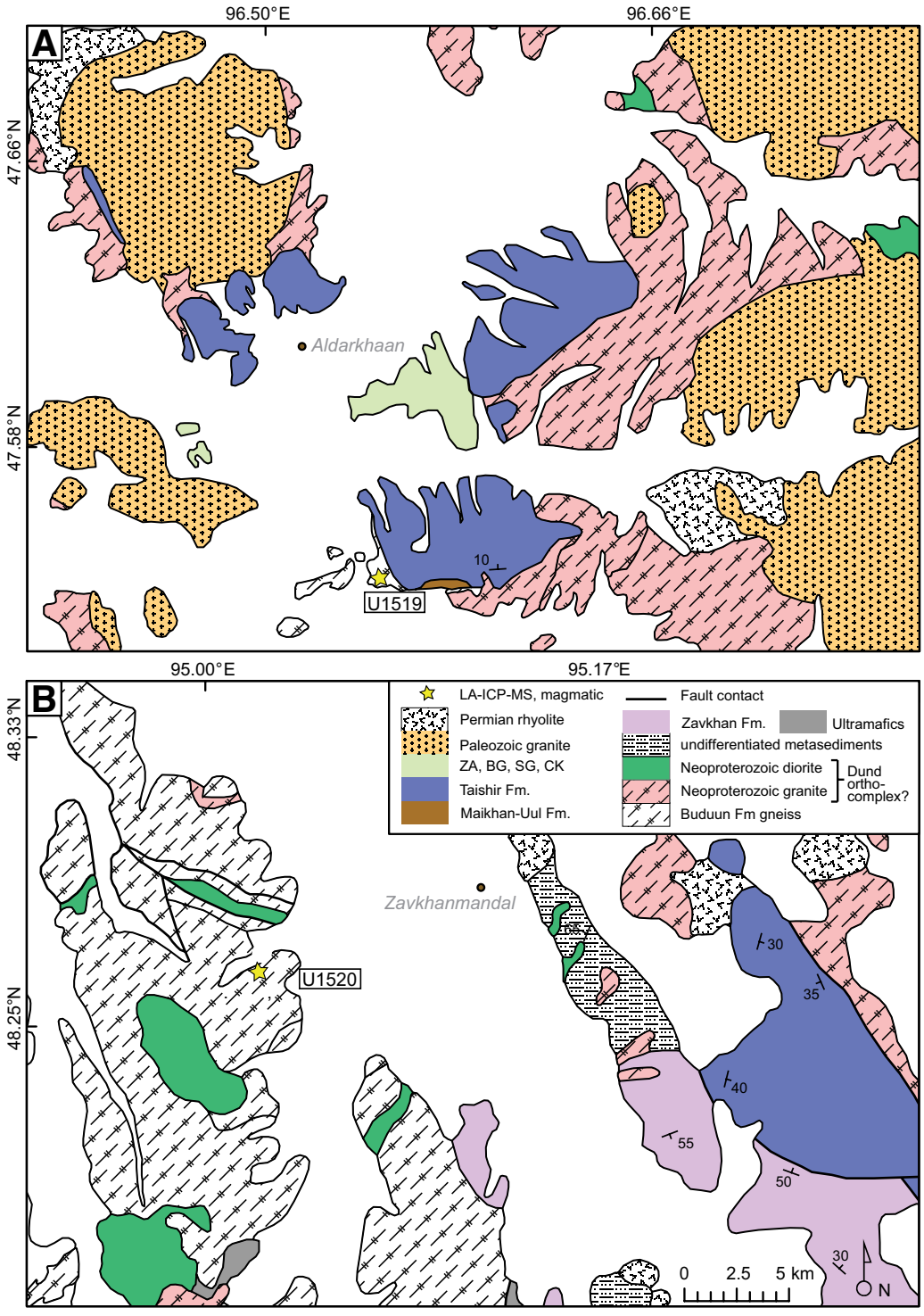

Figure 3. Geologic map of the northern Zavkhan terrane modified from 1:200,000 scale regional geologic map of Samozvantsen et al. (1981). (A) Geologic map of the Binder Khairkhan Mountain of the Aldarkhaan soum of the Zavkhan province, where granite gneiss sample U1519 was sampled. (B) Geologic map of the Zavkhanmandal soum, where granite gneiss sample U1520 was sampled. For detailed lithologic characteristics, see Kozakov et al. (2012b). Abbreviations: LA-ICP-MS—laser ablation–inductively coupled plasma–mass spectrometry; Fm. —formation; ZA—Zuun-Arts Formation; BG—Bayangol Formation; SG—Salaagol Formation; CK—Khairkhan Formation.

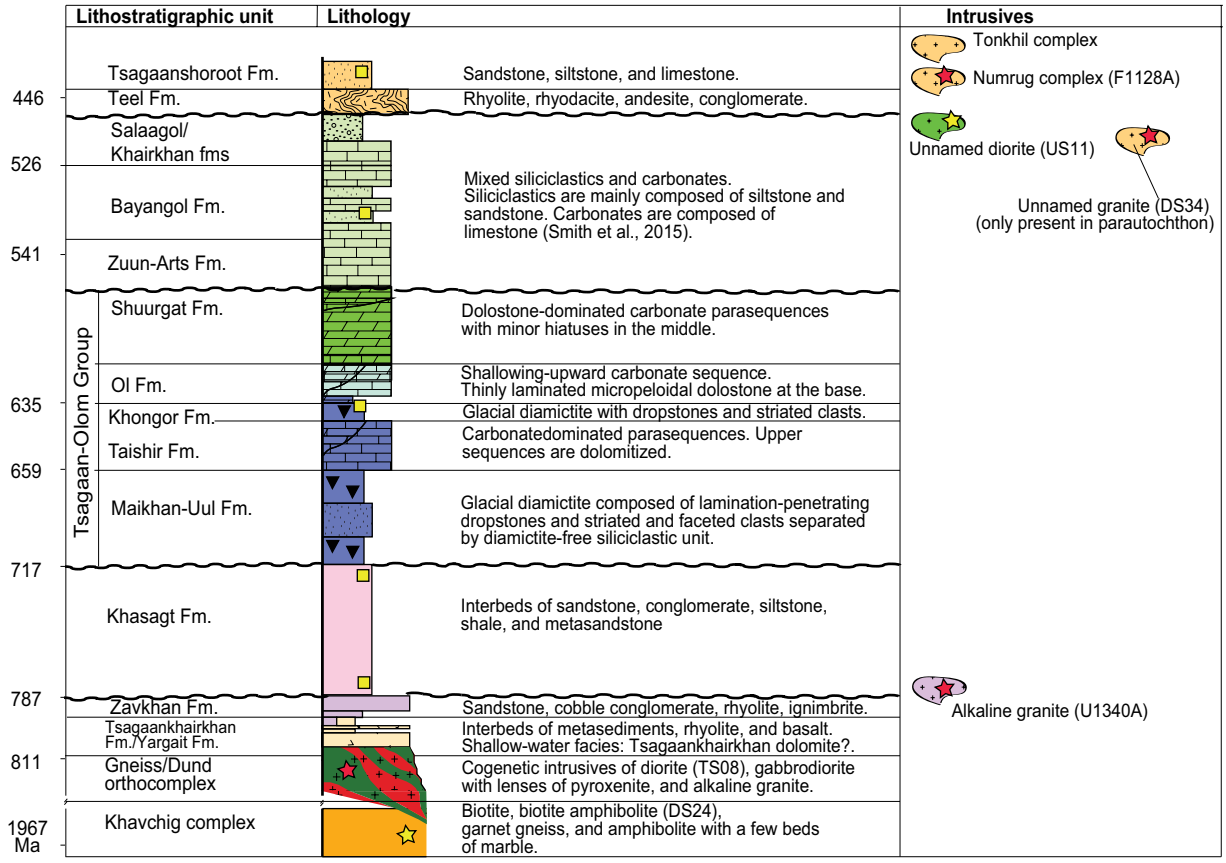

Figure 4. Generalized lithostratigraphy of the Zavkhan terrane. The units are color coded and labeled following Figure 2 (Fm.—formation). The stratigraphic horizons sampled for geochronology are labeled and magmatic sample numbers are included in parentheses.

All samples were first dated by laser ablation-inductively coupled plasma-mass spectrometry (LA-ICP-MS) U-Pb method and five samples were further analyzed by CA-ID-TIMS (Table 1; Figures 6–7). See the Data Repository[1] Item for U-Pb zircon geochronology methods.

RESULTS

Geochronologic results from the dated samples of the Zavkhan terrane are described from the oldest to the youngest. Petrographic observations (Fig. 8) are included if available along with the chemical compositions of zircon grains. Based on these new data, the ages of major structures and magmatic events are refined.

Sample DS24 is a micaceous granite gneiss in the Khavchig complex. The gneiss (Fig. 5F) is lepidoblastic, heteroblastic, granoblastic, and poikiloblastic in texture and is composed of plagioclase (35%–40%), quartz (25%–30%), micas (10%–15%), and potassium feldspar–perthite (10%–15%). Secondary minerals are represented by sericite, muscovite, chlorite, and epidote-zoisite and accessory minerals by opaque minerals (<5%), apatite, and zircon (Fig. 8A). LA-ICP-MS dates from 41 zircon cores and magmatic rims are 2469 ± 27–1888 ± 25 Ma (Figure A1 and Table A2 in the Data Repository). Dates from 26 grains (excluding dates from cores) are equivalent with a weighted mean of 1967 ± 13 Ma (mean square of weighted seviates (MSWD) = 1.3, probability of fit, p.o.f. = 0.15) (Fig. 6A).

Sample U1519 is light green granite gneiss in the Buduun Formation (Fig. 3A). The sample is directly overlain by the Maikhan-Uul Formation diamictite and Tsagaan-Olom Group carbonates (Figs. 5A, 5B). The lepidoblastic, heteroblastic, and granoblastic gneisses are composed of plagioclase (25%–30%), quartz (25%–30%), potassium feldspar (25%–30%), and biotite (5%–10%). Plagioclase is sericitized, corroded by quartz, and sometimes shows myrmekite intergrowths. Potassium feldspar is partly pelitized and includes poikiloblastic quartz and sometimes relicts of plagioclase and biotite. Biotite is often replaced by chlorite and rarely by epidote-zoisite. Accessory minerals are represented by apatite, titanite, zircon, and opaque minerals (Fig. 8B). LA-ICP-MS dates from 46 zircon cores and magmatic rims are 2523 ± 31–724 ± 15 Ma (Figure A2; Table A2); 4 grains have Paleoproterozoic inherited zircon cores. The rest of the grains are complicated mixtures of metamorphic and magmatic early Neoproterozoic zircons. The youngest four dates of 776 ± 30–724 ± 15 Ma are from rims. Because only one rim had a reliable zircon chemical composition, no weighted mean date was calculated for this metamorphic event (Fig. 6C).

Sample U1520 is pink granite gneiss in the Buduun Formation (Figs. 3B and 5D). U1520 was sampled from the same map unit dated by Kozakov et al. (2012b) at 856 ± 2 Ma and described as the basement of the

[1]GSA Data Repository Item 2016344, a summary of U-Pb zircon geochronology methods, related data, and cathodoluminescence images of zircon grains dated, including Tables A1–A3 and Figures A1–A21, is available at www.geosociety.org/pubs/ft2016.htm, or on request from editing@geosociety.org.

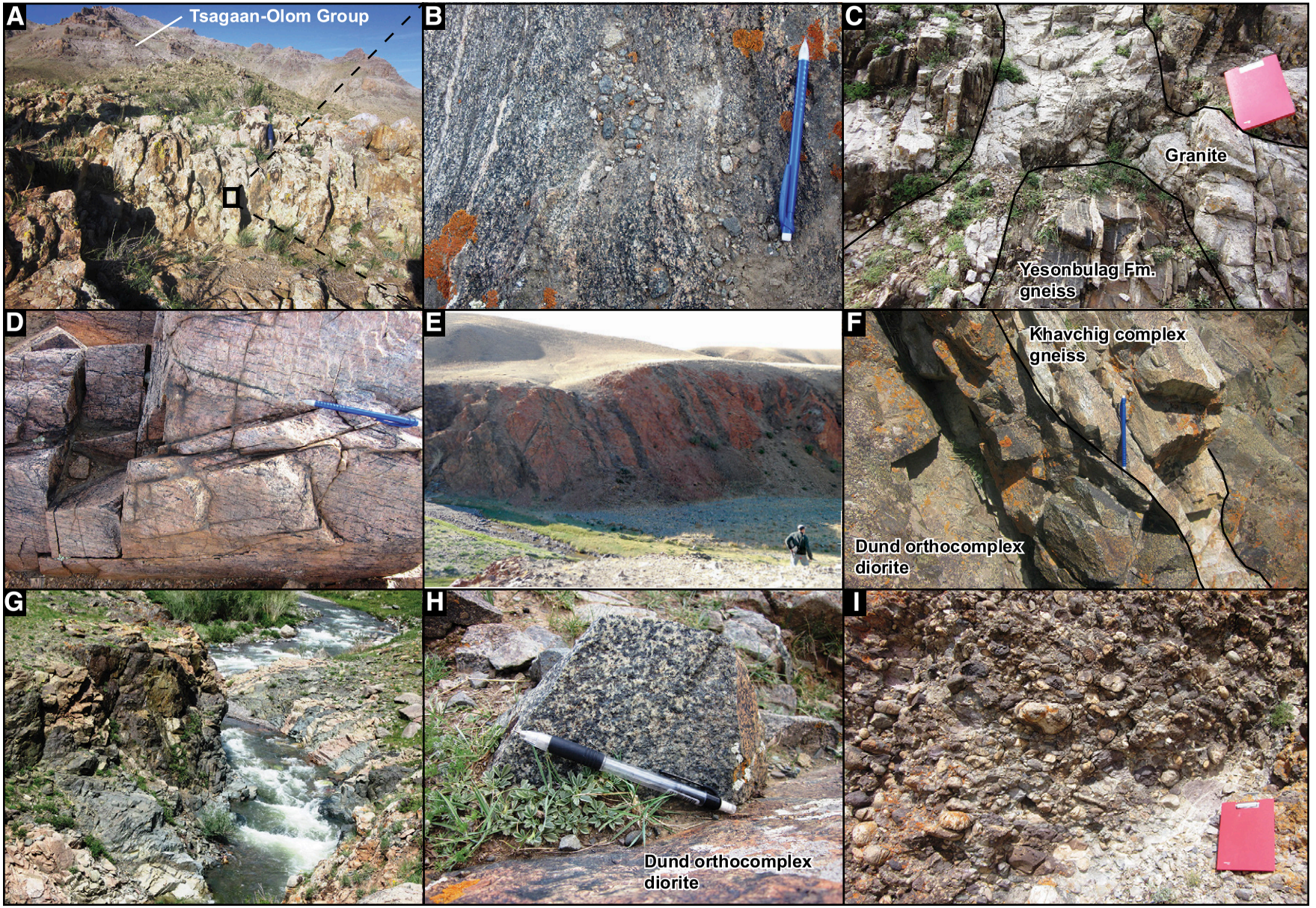

Figure 5. Field photographs of representative lithostratigraphic units of the Zavkhan terrane. (A) Granite gneiss exposed in Binder Khairkhan Mountain in Aldarkhaan soum of Zavkhan province with direct contact with dolomitized Tsagaan-Olom Group carbonates. View is to the east. Lower cliff is ~4 m tall. (B) Close-up of the granite gneiss where sample U1519 was taken. (C) Granite gneiss of the Yesonbulag Formation as exposed in Tsagaanchuluut Gorge. Later granite intrusions are highlighted. (D) Granite gneiss previously dated by Kozakov et al. (2012b) in the Zavkhanmandal soum of the Zavkhan province where sample U1520 was sampled. (E) The Dund orthocomplex as exposed in the mouth of the Orlogo Gorge. View is to the southeast. Note the extent of mafic dikes that are prevalent throughout the massif. Mafic dikes are ~3 m thick. (F) A view in the Urd Sharga Gorge of the Dund orthocomplex diorite that intrudes through the Khavchig complex granite gneiss. (G) The Dund orthocomplex diorite along with co-genetic granite as exposed in the Dund Sharga Gorge. The river is ~6 m wide. (H) The Dund orthochomplex diorite as exposed in the Dund Sharga Gorge. (I) The Zavkhan Formation cobble conglomerate as exposed in the western Khukh Davaa. The folder for scale is 24x32 cm.

TABLE 1. SUMMARY OF MAGMATIC AND DETRITAL SAMPLES DATED

Sample number	Age (Ma)	Uncertainty (±)	MSWD	p.o.f	Method	Latitude (°N)	Longitude (°E)	Interpretation	Formation and Rock Type	Location
Parautochthon										
DS24	1967	13	1.3	0.15	ICPMS	46.5451	95.6934	Crystallization	Khavchig complex muscovite-biotite gneiss	Daagan Del Range, Dund Sharga Gorge
TS08	811.36	0.24/0.45/0.94	0.6	0.67	CA-ID-TIMS	46.6380	95.8510	Crystallization	Dund orthocomplex hornblende diorite	Tsagaanchuluut Gorge
DS05	558	23	N.A.	N.A.	ICPMS	46.5010	95.6553	Maximum age	unnamed sandstone	Dund Sharga Gorge
US10	800	19	0.84	0.5	ICPMS	46.5257	95.9174	Crystallization	unnamed granite gneiss	Urd Sharga Gorge
US10	529	22	0.62	0.43	ICPMS	46.5257	95.9174	Metamorphic rim	unnamed granite gneiss	Urd Sharga Gorge
DS34	509.56	0.19/0.31/0.61	1.9	0.13	CA-ID-TIMS	46.6288	95.7774	Crystallization	unnamed granite	Dund Sharga Gorge
DS34	507.07	0.32/0.4/0.66	1.3	0.25	CA-ID-TIMS	46.6288	95.7774	Metamorphic rim	unnamed granite	Dund Sharga Gorge
U12001	509.3	0.42/0.49/0.72	1.3	0.27	CA-ID-TIMS	46.6272	95.7161	Crystallization	Yesonbulag granite gneiss	Gurvan Khairkhan Mountain
US11	496	7	1.14	0.25	ICPMS	46.5234	95.9214	Crystallization	unnamed biotite-hornblende-quartz diorite	Urd Sharga Gorge
Autochthon										
U1519	N.A.	N.A.	N.A.	N.A.	ICPMS	47.5445	96.5492	N.A.	Buduun granite gneiss	Binder-Khairkhan Mountain, Aldarkhaan soum
U1520	839	11	1.2	0.15	ICPMS	48.2713	95.0245	Crystallization	Buduun granite gneiss	Zavkhanmandal soum
U1331	778	37	N.A.	N.A.	ICPMS	47.1181	95.2778	Maximum age	Khasagt sandstone	western Khukh-Davaa
U1340A	770.31	0.23/0.43/0.89	1.8	0.12	CA-ID-TIMS	46.8842	96.5595	Crystallization	unnamed alkaline granite	Tsagaanchuluut soum
DS69	733	34	N.A.	N.A.	ICPMS	46.7363	95.8335	Maximum age	Khasagt arkose	Dund Sharga Gorge
U1121-17.5	646	23	N.A.	N.A.	ICPMS	46.6630	96.2554	Maximum age	Khongor siltstone	Khongor Range
F1128B	465	15	N.A.	N.A.	ICPMS	46.7841	95.7332	Maximum age	Teel conglomerate	Khasagt Khairkhan Range
F1128A	442.1	0.19/0.28/0.54	1.5	0.18	CA-ID-TIMS	46.7841	95.7332	Crystallization	Numrug complex granite	Khasagt Khairkhan Range
U1127-1	341	40	N.A.	N.A.	ICPMS	46.8878	95.7278	Maximum age	Teel sandstone	Salaa Gorge
E1105-35.3	533	18	N.A.	N.A.	ICPMS	46.84342	95.77497	Maximum age	Bayangol siltstone	Salaa Gorge
F1121-25	721	19	N.A.	N.A.	ICPMS	46.7068	96.31077	Maximum age	Bayangol sandstone	Bayan Gorge
E1326	695	38	N.A.	N.A.	ICPMS	46.62258	96.65673	Maximum age	Bayangol quartz pebble conglomerate	Southern Khukh Davaa
E1336-41	722	49	N.A.	N.A.	ICPMS	47.0473	95.48747	Maximum age	Khairkhan conglomerate	Southern Khukh Davaa

Note: MSWD—mean square of weighted deviates; p.o.f.—probability of fit; N.A.—not applicable. ICP-MS—inductively coupled plasma-mass spectrometry; CA-ID-TIMS—chemical abrasion-isotope dilution-thermal ionization mass spectrometry.

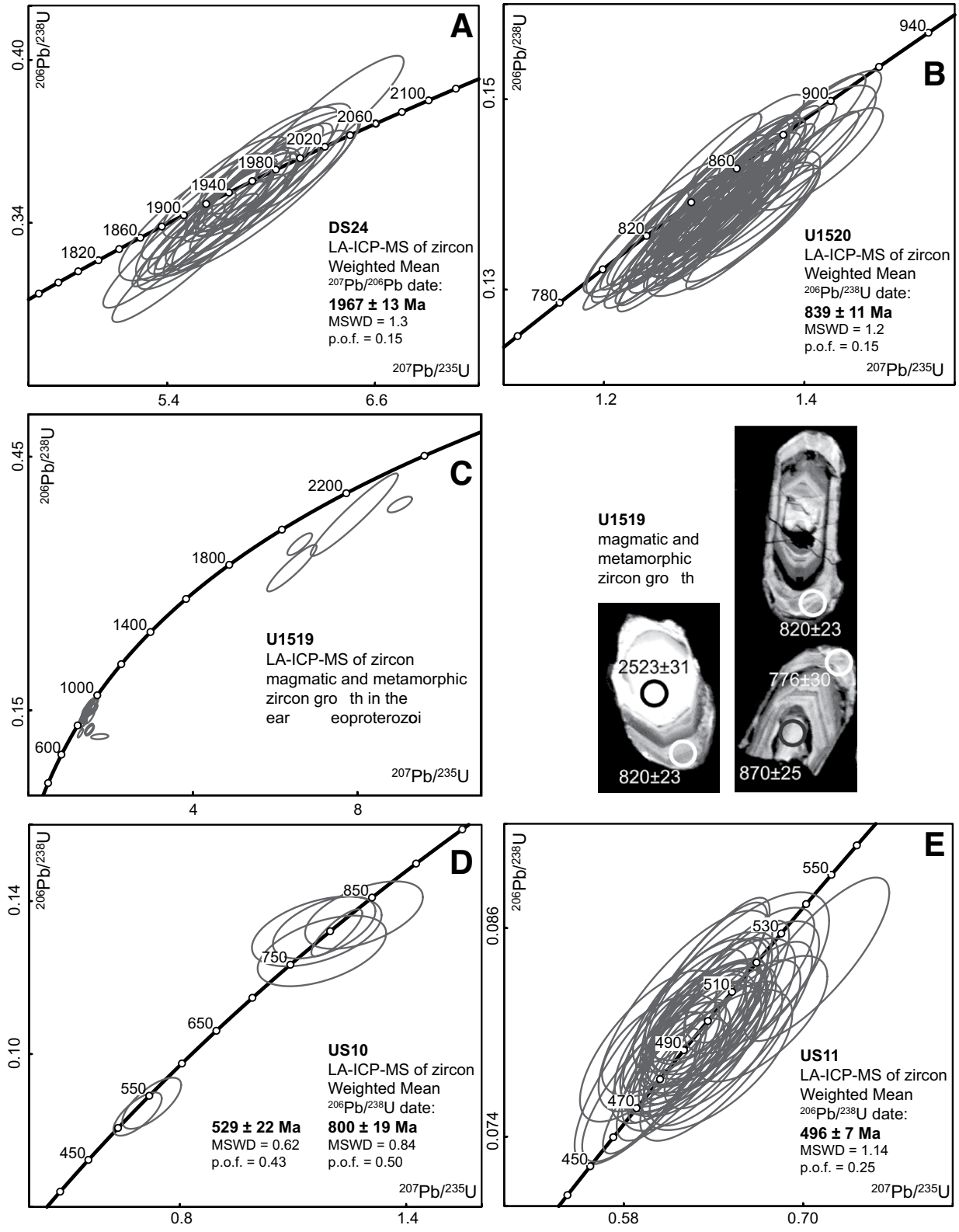

Figure 6. Concordia diagrams of the dated samples analyzed by LA-ICP-MS (laser ablation–inductively coupled plasma–mass spectrometry). MSWD—mean square of weighted deviates; p.o.f.—probability of fit. (A) A granite gneiss (U1520) dated in the Zavkhanmandal soum of the Zavkhan province from a previously dated complex by Kozakov et al. (2012b). (B) A granite gneiss (DS24) dated in the Khavchig complex. (C) A biotite-hornblende-quartz diorite (U.S.11) dated in the Urd Sharga Gorge. (D) A granite gneiss (U.S.10) dated in the Urd Sharga Gorge. (E) A granite gneiss (U1519) dated at Khairkhan Mountain in the Aldarkhaan soum of the Zavkhan province. Results yield complicated mixture of metamorphic and magmatic zircon growth in the early Neoproterozoic and hence cathodoluminescence images of representative zircon grains are shown.

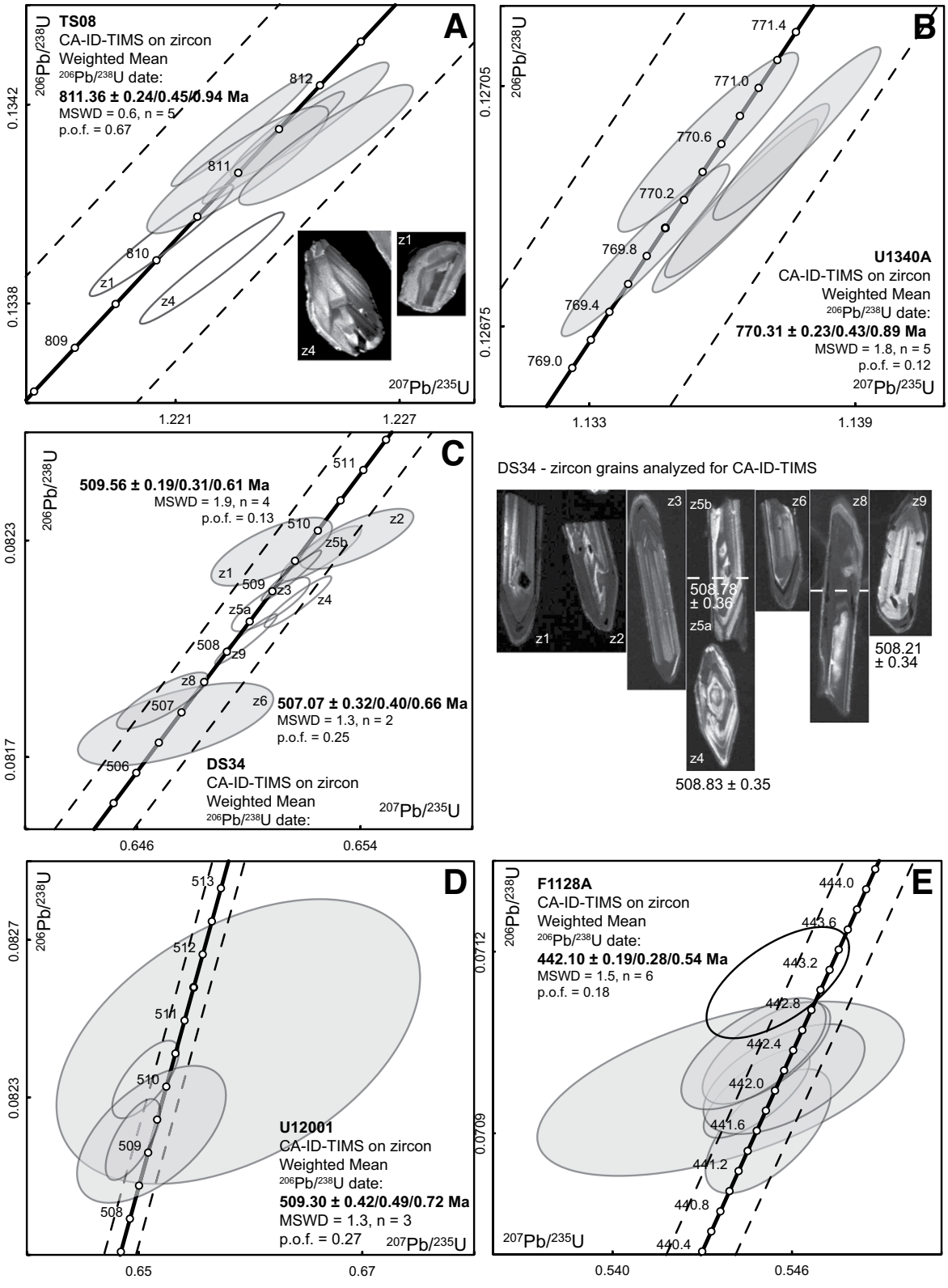

Figure 7. Concordia diagrams of the samples analyzed by CA-ID-TIMS (chemical abrasion–isotope dilution–thermal ionization mass spectrometry). MSWD—mean square of weighted deviates; p.o.f. —probability of fit. (A) A granite (F1128B) taken along a fault zone in Salaa Gorge. (B) A granite gneiss (U12001) taken in the Yesonbulag Formation in the western Dund Sharga Gorge. (C) A hornblende diorite (TS08) of the Dund orthocomplex sampled in Tsagaanchuluut Gorge. The two zircon grains that yielded younger dates have thin white rims (metamorphic?), which may have affected the final result. (D) An alkaline granite (U1340A) sampled in Tsagaanchuluut soum. (E) A granite (DS34) sampled in the Dund Sharga Gorge in the parautochthonous region. Two weighted mean dates were calculated to constrain tectonomagmatic events recorded within the zircon grains.

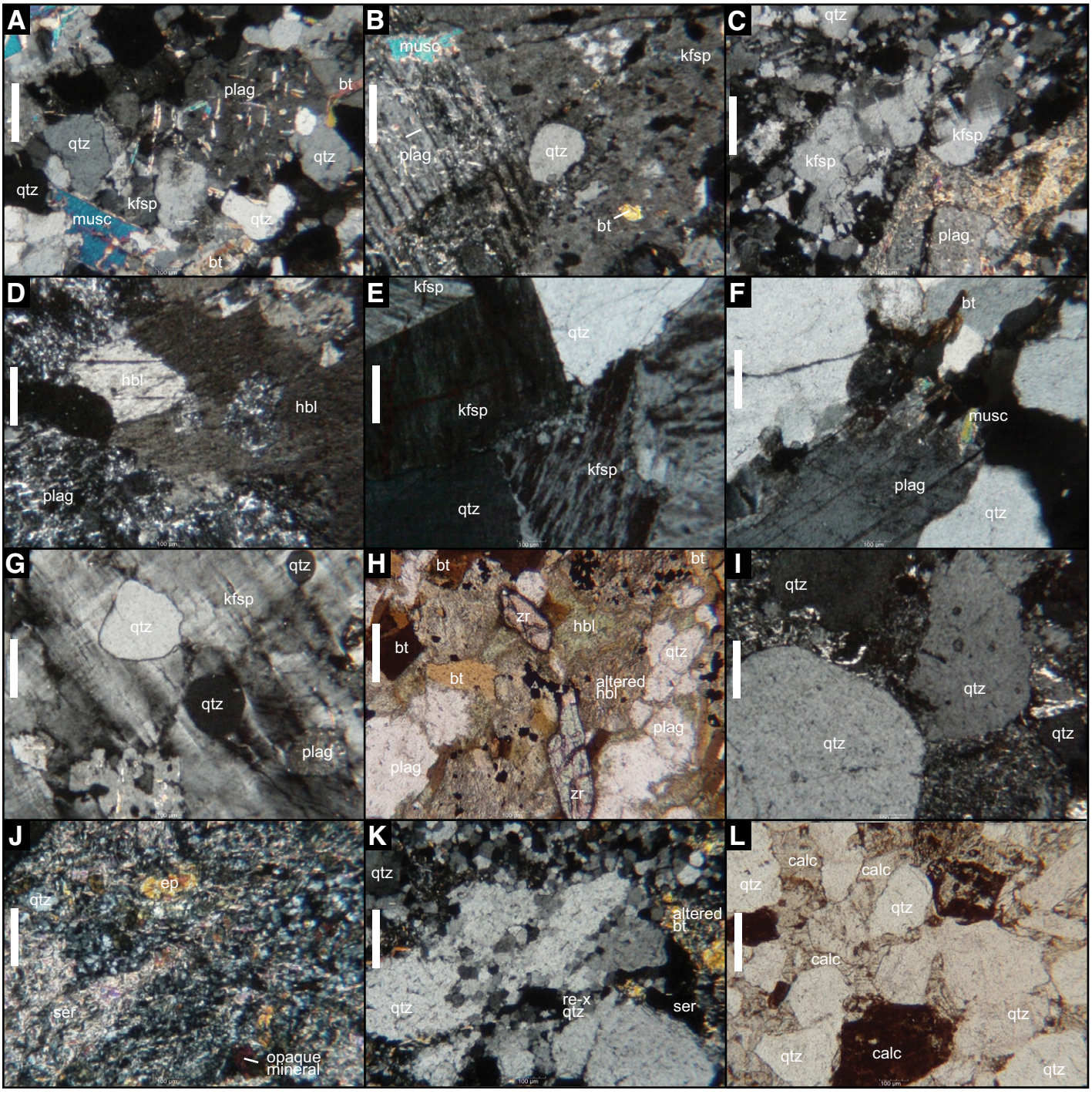

Figure 8. Photomicrographs of the representative lithostratigraphic units. A-G and I-K were taken in crossed polarized light and H and L were taken in plane polarized light. Qtz—quartz, kfsp—potassium feldspar, calc—calcite, plag—plagioclase, musc—muscovite, bt—biotite, ser—sericite, zr—zircon, hbl—hornblende, ep—epidote, and re-x—recrystallized. Scale bar is 200 µm. (A) Micaceous granite gneiss (DS24). Poikiloblastic texture is shown by quartz grain at the boundary between plagioclase and quartz. (B) Granite gneiss (U1519). Poikiloblastic texture is shown by quartz included in plagioclase crystal. (C) Granite gneiss (U1520). Poikiloblastic texture is shown by small quartz crystals. Plagioclase is sericitized. (D) Hornblende diorite (TS08). Abundance of hornblende is represented by large hornblende crystals. (E) Coarse crystalline alkaline granite (U1340A). Subhedral to euhedral potassium feldspar crystals are shown with quartz crystals. (F) Plagiogranite (U.S.10). Faint polysynthetic twinning of plagioclase crystals is shown. (G) Granite gneiss (U12001). Poikiloblastic texture is represented by quartz grains included in large potassium feldspar crystal. Plagioclase crystals are sericitized. (H) Biotite-hornblende-quartz diorite (U.S.11). Large zircon crystals are shown by high relief and representative crystal habit. (I) Arenite (U1331). Quartz grains are well-rounded but poorly sorted. Matrix is composed of sericite and opaque minerals. J and K are photomicrographs of metasandstone (DS05). (J) Epidotized, silicified, and sericitized sandstone. (K) Large quartz crystals are shown along with recrystallized quartz and silicified matrix. (L) Lithoarenite (U1127–1). Quartz grains are poorly rounded and matrix is composed of mostly carbonate.

Zavkhan terrane (Samozvantsen et al., 1981). The porphyroblastic and lepidoblastic, heteroblastic,granoblastic granite gneiss is composed of microcline perthite (35%–40%), plagioclase (20%–25%), biotite (<5%), and quartz (30%–35%). Micropoikiloblastic texture is common represented by quartz included in potassium feldspar. Biotite is often altered to sericite, muscovite and opaque minerals. Recrystallized quartz is also common (Fig. 8C). LA-ICP-MS dates from 61 zircon grains are 886 ± 28–795 ± 29 Ma (Figure A3; Table A2). Ages from 54 dates are equivalent, with a weighted mean of 839 ± 11 Ma (MSWD = 1.2, p.o.f. = 0.15; Fig. 6B).

Sample TS08 is dark green, coarsely crystalline hornblende diorite in the Dund orthocomplex (Figs. 2 and 5H). It has hypidiomorphic granular in texture and is composed of plagioclase (50%–55%), hornblende (35%–40%), and quartz (<5%). Secondary minerals are represented by sericite and pelite and accessory minerals by opaque minerals (<5%). Plagioclase is subhedral and polysynthetically twinned, whereas hornblende is euhedral to subhedral (Fig. 8D). LA-ICP-MS dates from 59 zircon grains are 872 ± 35–750 ± 31 Ma (Figure A4; Table A2). The 5 oldest of 7 zircon grains analyzed by CA-ID-TIMS yielded equivalent dates with a weighted mean of 811.36 ± 0.24/0.45/0.94 Ma [Errors on the weighted mean dates are given as ± x/y/z, where x is the internal error based on analytical uncertainties only, including counting statistics, subtraction of tracer solution, and blank and initial common Pb subtraction, y includes the tracer calibration uncertainty propagated in quadrature, and z includes the ^{238}U decay constant uncertainty propagated in quadrature] (MSWD = 0.6, p.o.f. = 0.67); 2 other grains yielded dates of 809.91 ± 0.52 and 810.23 ± 0.52 Ma (Fig. 7A; Table A1).

Sample U1331 is dark purple, coarse- to medium-grained arenite in the Khasagt Formation. At this locality, the unit directly overlies the Zavkhan Formation rhyolites. The psammitic arenite is clast dominated (85%–90%) and is composed of well-rounded and medium-sorted quartz grains (0.1–1.2 mm; 90%–95%) that are cemented by sericite (0.6–1 mm; 6%–8%) and opaque minerals (0.2–0.3 mm; 1%–2%) (Fig. 8I). LA-ICP-MS dates from 112 detrital zircon grains are 2930 ± 70–778 ± 33 Ma (Figure A5; Table A3). Prominent age peaks are at 1000–750 and 1900–1780 Ma (Fig. 9).

Sample U1340A is coarse-grained alkaline granite that intrudes the Zavkhan Formation. This granite was previously dated with two large multigrain bulk zircon fractions at 755 ± 3 (Yarmolyuk et al., 2008). The granite is composed of potassium feldspar–perthite (55%–60%), quartz (25%–30%), plagioclase (5%–10%), and biotite (<5%). Potassium feldspar is subhedral, often pelitized, and corroded by quartz. Plagioclase is subhedral and lightly sericitized. Pseudomorphs of biotite and hornblende that are completely altered by chlorite, opaque minerals, and quartz are present. Accessory minerals are apatite, titanites and/or sphene, and zircon (Fig. 8E). Microfractures within the granite are commonly filled by sericite, quartz, opaque minerals, and hydrous ferric oxides. LA-ICP-MS dates from 25 zircon grains are 872 ± 31–670 ± 31 Ma (Figure A6; Table A2). CA-ID-TIMS dates from 5 grains are equivalent with a weighted mean of 770.31 ± 0.23/0.43/0.89 Ma (MSWD = 1.8, p.o.f. = 0.12) (Fig. 7B; Table A1).

Sample DS69 is pale gray, coarse-grained lithic sandstone in the Khasagt Formation. This unit directly overlies a local fault bordering with the Yargait Formation. The sandstone is clast dominated (85%–90%), and is cemented by carbonate, sericite, quartz, and chlorite. Clasts are often angular, poorly sorted, and are mainly composed of rhyolite (1–4.6 mm; 60%–65%). LA-ICP-MS dates from 60 detrital zircon grains are 1998 ± 25–733 ± 34 Ma. A prominent peak in the age spectra occurs at 850–700 Ma (Fig. 9; Figure A7; Table A3).

Sample U1121–17.5 is shaly siltstone in the Khongor Formation. The sample was sampled in the matrix of the Khongor Formation diamictite, 17.5 m above the base. LA-ICP-MS dates from 70 detrital zircon grains are 2623 ± 57–646 ± 23 Ma. Prominent age peaks are at 900–700 and 2100–2000 Ma (Fig. 9; Table A3).

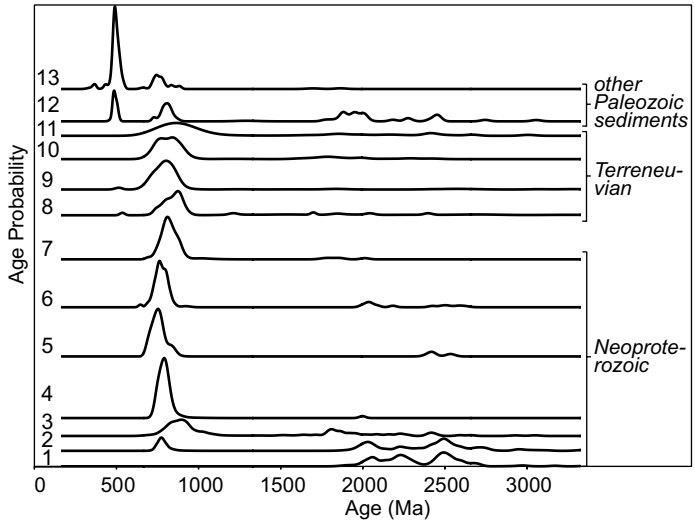

Figure 9. Normalized probability plots of U-Pb dates obtained by laser ablation–inductively coupled plasma–mass spectrometry from zircon grains of the detrital samples of the Zavkhan (1, 2), Khasagt (3, 4), Maikhan-Uul (5), Shuurgat (7), Bayangol (8–10), Khairkhan (11), and Teel (12, 13) Formations of the Zavkhan terrane. 1-U1333, 2-U1214, 3-U1331, 4-DS69, 5-F1203–272.1, 6–U1121–17.5, 7-F1206–146.1, 8-E1105–35, 9-F1121–25, 10-E1326, 11-E1336–41, 12–F1128B, and 13-U1127–1. For U1333, U1214, F1203–272.1, and F1206–146.1 data, see Bold et al. (2016).

Sample E1105–35.3 is siltstone in the Bayangol Formation. The sample was collected as possibly being an ash, but dates indicate that zircon grains are detrital. LA-ICP-MS from 31 zircon grains are 2401 ± 25–533 ± 18 Ma (Figure A9; Table A3). Age peaks are at 920–760 Ma (Fig. 9).

Sample F1121–25 is ~10-cm-thick sandstone from just below pink stromatolite marker beds in Member BG3 of the Bayangol Formation. This sample was collected while measuring section F1121 in the Bayan Gorge. LA-ICP-MS dates from 29 zircon grains are 2419 ± 55–721 ± 19 Ma (Figure A10; Table A3). Age peaks are at 850–750 Ma (Fig. 9).

Sample E1326 is white to pink quartz-pebble conglomerate of Member BG6 of the Bayangol Formation. LA-ICP-MS dates from 69 zircon grains are 2423 ± 56–695 ± 38 Ma (Figure A11; Table A3). Age peaks are at 900–720 Ma (Fig. 9).

Sample E1336–41 is poorly sorted pebble conglomerate in the Khairkhan Formation. This sample was collected in measured section E1339. At this locality, the Salaagol Formation is absent, and the Khairkhan Formation directly overlies the Bayangol Formation. LA-ICP-MS dates from 112 zircon grains are 2988 ± 53–722 ± 49 Ma (Figure A12; Table A3). Age peaks are at 950–720 Ma (Fig. 9).

Sample DS05 is pink gray, epidotized, sericitized, and silicified lithic metasandstone in metasiliciclastics in an undifferentiated unit in the southern Dund Sharga Gorge. The metasandstone is blastopsammitic and schistose in texture and composed of clasts (50%–55%) of quartz (<1 mm; 40%–45%), altered color minerals that are characterized by epidote and sericite (~0.8; <5%), feldspar (<0.1 mm, <5%), apatite (<0.15 mm; <1%), opaque minerals (<0.15 mm; <1%), and rhyolite (<1.8 mm; <5%). Quartz clasts are partly recrystallized forming microgranoblastic aggregates. Cements (45%–50%) are composed of epidote-zoisite (10%–15%), quartz (10%–15%), and sericite (15%–20%) (Figs. 5J, 5K). LA-ICP-MS dates from 12 zircon grains are 689 ± 71–558 ± 23 Ma (Figure A13; Table A3).

Sample U.S.10 is light gray granite gneiss (mapped as Paleoproterozoic by Togtokh et al. (1995)). It is lepidoblastic andgranoblastic in texture and composed of plagioclase (35%–40%), microcline (5%–10%), quartz (30%–35%), biotite (5%–10%), and muscovite (<5%). Micropoikiloblastic texture is often shown by small quartz grains included in microcline. Secondary minerals are sericite, chlorite, and hydrous iron oxides. Accessory minerals are represented by opaque minerals (<1%), apatite (1%–2%), titanite (<1%), zircon (1%–2%), and garnet (<1%) (Fig. 5F). LA-ICP-MS dates from 23 zircon cores and magmatic rims are 2629 ± 51–522 ± 28 Ma (Figure A14; Table A2). Excluding the cores, the dates on magmatic rims are equivalent with a weighted mean of 800 ± 19 Ma (MSWD = 0.84, p.o.f. = 0.5). Dates from metamorphic rims on 2 grains are equivalent with a weighted mean of 529 ± 22 Ma (MSWD = 0.62, p.o.f. = 0.43) (Fig. 6D).

Sample DS34 is white, coarsely crystalline unnamed granite that intrudes the gneissose strata of the parautochthon. LA-ICP-MS dates from 33 zircon cores and magmatic rims are 2900 ± 54–461 ± 17 Ma (Table A2). 8 zircon grains were analyzed by CA-ID-TIMS method, with 2 fragments from one of the grains being analyzed. The 2 youngest dates are equivalent with a weighted mean of 507.07 ± 0.32/0.40/0.66 Ma (MSWD = 1.3, p.o.f. = 0.25). The Th/U ratios of these grains are <0.1. The next oldest 3 dates are 508.21 ± 0.34–508.83 ± 0.35 Ma. The next oldest 4 dates are equivalent with a weighted mean of 509.56 ± 0.19/0.31/0.61 Ma (MSWD = 1.9, p.o.f. = 0.13) (Fig. 7C; Figure A15; Table A1).

Sample U12001 is biotite granite gneiss (Fig. 5C) in the Yesonbulag Formation. The gneiss is lepidoblastic and granoblastic in texture and composed of microcline-perthite (30%–35%), plagioclase (20%–25%), quartz (25%–30%), biotite (5%–10%), and muscovite (<5%). Microcline perthite is subhedral to anhedral, weakly pelitized, shows micropoikiloblastic texture by inclusion of quartz, and hosts micrograins of plagioclase, and biotite. Plagioclase is often subhedral, altered to pelite and sericite, sometimes replaced by potassium feldspar displaying myrmekite texture, corroded by quartz, and includes quartz micropoikiloblasts. Quartz is recrystallized and biotite is often replaced by muscovite (Fig. 8G). LA-ICP-MS dates from 18 zircon grains (cores and magmatic rims) are 1993 ± 58–465 ± 23 (Figure A16; Table A2). Of the 4 zircon grains analyzed by CA-ID-TIMS, 3 are equivalent with a weighted mean of 509.30 ± 0.42/0.49/0.72 Ma (MSWD = 1.3, p.o.f. = 0.27). The other date is 510.11 ± 0.48 Ma (Fig. 7D; Table A1).

Sample U.S.11 is dark green unnamed biotite-hornblende-quartz diorite (mapped as middle Paleoproterozoic in age on geologic map by Togtokh et al. (1995)). It is hypidiomorphic granular in texture and composed of plagioclase (45%–50%), hornblende (15%–20%), biotite (10%–15%), and quartz (10%–15%). Plagioclase is subhedral, zonal, polysynthetically twinned, and sometimes deformed. Hornblende is euhedral to subhedral, and often replaced by actinolite, tremolite, chlorite and reddish brown biotite. Accessory minerals are represented by titanite, apatite, zircon, and opaque minerals (Fig. 8H). LA-ICP-MS dates from 42 zircon grains are 541 ± 20–476 ± 18 Ma (Figure A17; Table A2). 39 dates are equivalent with a weighted mean of 496 ± 7 Ma (MSWD = 1.14, p.o.f. = 0.25) (Fig. 6E).

Sample F1128B is conglomerate along a major fault zone in the Teel Formation (Fig. 2). LA-ICP-MS dates from 56 zircon grains are 3056 ± 28–474 ± 30 Ma (Figure A18; Table A3). Age peaks are at 550–450, 1050–800, 2100–1900, and 2550–2450 Ma (Fig. 9).

Sample F1128A is pink unnamed granite along a major fault zone (Fig. 2). LA-ICP-MS dates from 29 zircon grains are 445 ± 26 Ma and 372 ± 14 Ma. CA-ID-TIMS dates from 7 grains were analyzed (Figure A19; Table A2). The 6 youngest dates are equivalent with a weighted mean of 442.10 ± 0.19/0.28/0.54 Ma (MSWD = 1.5, p.o.f. = 0.18). The other date is 443.07 ± 0.45 Ma (Fig. 7E; Table A1).

Sample U1127–1 is pale brown litharenite in the Teel Formation. The sample is psammitic in texture and clast dominated (80%–85%); the clasts are composed of quartz (~0.5 mm; 75%–80%), potassium feldspar (~0.4 mm; <5%), microquartzite (5%–10%), micas (<0.3 mm; 1%–2%), and limestone (5%–10%) and are cemented by mostly carbonate (10%–12%) and rarely hydrous ferric oxide and opaque minerals (2%–3%) (Fig. 8L). LA-ICP-MS dates from 89 zircon grains are 1698 ± 81–361 ± 20 Ma (Figure A20; Table A3).Only one zircon grain yielded a date younger than 432 ± 18 Ma; this needs to be analyzed by CA-ID-TIMS before giving it any significance. Age peaks are at 650–500 Ma and 900–750 Ma (Fig. 9).

DISCUSSION

Tectonic significance of U-Pb zircon geochronology

Age constraints on magmatism and metamorphism

The age of the Zavkhan terrane basement has long been considered to be ca. 1800 Ma from a bulk zircon fraction TIMS $^{207}Pb/^{206}Pb$ date from the Khavchig complex (Burashnikov, 1990). We suggest that ca. 507 Ma metamorphic rims compromised the previous date and that our LA-ICP-MS date of 1967 ± 13 Ma (Fig. 6A) from zircon rims of Khavchig complex gneiss is more accurate. This difference is significant because the basement was previously correlated with 1820 ± 27 Ma basement of the Baidrag terrane (SHRIMP U-Pb zircon; Demoux et al., 2009a), which contributed to the assumption that the two terranes were one (e.g., Wilhem et al., 2012; Windley et al., 2007).

It was also previously unclear if the Altai allochthon and the Zavkhan terrane shared the same Proterozoic basement (Bold et al., 2016; Bucholz et al., 2014; Kozakov et al., 2012b); however, we show that diorite of the Dund orthocomplex intruded the Khavchig complex (Fig. 5F) and underlies the Yargait and Shandiinnuruu Formations, which are depositionally overlain by the Zavkhan Formation. The Dund orthocomplex (Ruzhentsev and Burashnikov, 1996) consists of cogenetic massive intrusions of diorite (Fig. 5H), gabbrodiorite, gabbro, and alkaline granite (Fig. 5G) that are particularly well-exposed in the Khoid Sharga Gorge (Fig. 5E) with mutually crosscutting relationships. The CA-ID-TIMS date of 811.36 ± 0.24 Ma from the diorite (sample TS08, Fig. 7A) is interpreted to reflect magmatism and crystallization of mingling mafic and felsic end-members of the Dund orthocomplex in the Zavkhan terrane. In the Nomgon, Dund Sharga, and Urd Sharga Gorges, the Dund orthocomplex directly feeds rhyolite domes and dolerite sills (Figs. 2 and 4). The overlying Shandiinnuruu Formation was defined based on more interbeds of volcanic rocks whereas the definition of the Yargait Formation was based on prevalence of metasedimentary rocks (Togtokh et al., 1995). Recognizing that these units interfinger and represent lateral facies change rather than temporally discrete stratigraphic units, the entire volcanic strata and metasedimentary units above the Dund orthocomplex are lumped into the Yargait Formation (Fig. 4). Therefore, the autochthon and parautochthon were conjoined by at least 811.36 ± 0.24 Ma. Detrital zircon data discussed below further here demonstrate that overlap assemblages on the autochthon and parautochthon have the same basement sedimentary sources (Fig. 9).

On the parautochthonous basement, two other orthogneiss samples have crystallization ages of 800 ± 19 Ma (sample U.S.10, with a metamorphic zircon rim growth at 529 ± 22 Ma, Fig. 6D) and 509.30 ± 0.42 Ma (sample U12001, Fig. 7D). The 800 ± 19 Ma age provides another tie with the autochthon. On the contrary, the Buduun Formation gneiss on the autochthonous Zavkhan terrane yielded a crystallization age of 839 ± 11 Ma (sample U1520, Fig. 6B) and is intruded by undeformed granite and gabbroic dikes, possibly correlative with the Dund orthocomplex. Both the gneiss and the granite gabbro intrusions are unconformably overlain

by low-grade Cryogenian strata (Fig. 3). These data suggest that there was a metamorphic event in the northern portion of the Zavkhan terrane between 839 ± 11 and 811.36 ± 0.24 Ma.

Rhyolites of the Zavkhan Formation have previously been dated between ca. 802 and 787 Ma (Bold et al., 2016). The tectonic setting of these volcanic rocks has been debated in the literature (Ilyin, 1990; Levashova et al., 2010; Ruzhentsev and Burashnikov, 1996); however, the zircon chemical compositions of the Zavkhan Formation samples that we dated are consistent with an arc origin (Yang et al., 2012; Fig. A21). North of the Zavkhan River, the Zavkhan Formation is intruded by 770.31 ± 0.23 Ma alkaline granites (sample U1340A, Fig. 7B), which have been interpreted to be rift related based on whole-rock geochemistry (Yarmolyuk et al., 2008). Therefore, we suggest that the 770.31 ± 0.23 Ma alkaline granites mark the beginning of rifting, which was responsible for the fault-bound deposition of the Khasagt Formation sediments and possibly associated with the few-tens-of-meters-thick basaltic flows above the Zavkhan Formation in the Ulaanbulag Gorge (Fig. 2).

Detrital zircon dates reveal a magmatic gap between ca. 770 and 580 Ma (Fig. 9), which along with the Cryogenian to Ediacaran stratigraphic architecture (Bold et al., 2016), verify the development of a rifted passive margin. Dates between ca. 581 and 558 Ma, revealed in unnamed metasediments (sample DS05) in the south Dund Sharga Gorge, record arc magmatism in the Lake terrane, whereas the youngest date of 533 ± 18 Ma in the siliciclastics of the Bayangol Formation (sample E1105–35.3) support arrival of the arc. Cambrian plutonism is present on the parautochthon, where we dated a granite at 509.56 ± 0.19 Ma with a metamorphic zircon rim growth at 507.07 ± 0.32 Ma (sample DS34, Fig. 7C). This granite intruded not only the 1967 ± 13 Ma Khavchig complex, but also an 800 ± 19 Ma gneiss with a metamorphic zircon rim growth at 529 ± 22 Ma (sample U.S.10), and a 509.30 ± 0.42 Ma gneiss (sample U12001). We therefore suggest that ca. 509–507 Ma granites are synorogenic. Metamorphic grade decreases rapidly to the north with greenschist metamorphism and tight folding south of the fault 2, Fig. 2) separating the Yargait Formation from the weakly folded Tsagaan-Olom Group.

In addition to massive diorite and granodiorite plutons of the Dund orthocomplex, smaller plugs of diorite are present in the southern portion of the Zavkhan terrane (Fig. 2). Previously, these were all mapped as part of the Dund orthocomplex; however, our data provide evidence that at least some of these are Cambrian (496 ± 7 Ma (sample U.S.11, Fig. 6E)). These intrusions lack the gneissic fabric present in the Yesonbulag Formation granite gneiss and tightly constrain the age of metamorphism in the parautochthonous region to between 507.07 ± 0.32 and 496 ± 7 Ma.

The age of the Numrug complex is now determined to be 442.10 ± 0.19 Ma (sample F1128A, Fig. 7E). This is associated with Late Ordovician to Silurian extensional tectonism responsible for forming grabens that are filled with bimodal volcanism and sedimentary strata of the Teel Formation (Kilian et al., 2016).

Age constraints on faulting

With better geologic and geochronologic characterization of the main lithostratigraphic units of the Zavkhan terrane, the major structures can now be discussed in more detail with greater confidence. The parautochthonous basement of the Zavkhan terrane is bound to the south by a large fault (fault 1, Fig. 2) that separates Khavchig complex gneiss to the north with an undifferentiated metavolcanic-sedimentary unit (sample DS05) to the south. The few zircon grains retrieved from DS05 yielded dates of ca. 581–558 Ma (Table A3) that are indistinguishable from plagiogranites dated in both the Dariv and Khantaishir ophiolites (Khain et al., 2003) of the Lake terrane. We suggest that these units are distal foreland equivalent to the Terreneuvian foreland on the Zavkhan terrane, but more dominated by sedimentary sources from the upper plate, whereas the foreland on the autochthon received most of its sediment from the autochthon. To the west of the Urd Sharga Gorge, north of fault 1, a Paleozoic alkaline granite intrudes the Khavchig complex gneiss. However, a strip of the Middle Devonian Tsagaanshoroot Formation is present along the fault zone, which suggests that although this structure defines a Cambrian suture, it was reactivated after the Middle Devonian.

In the Dund Sharga, Khoid Sharga, and Nomgon Gorges, a major fault (fault 2, Fig. 2) separates tightly folded metasedimentary and volcanic rocks of the Yargait Formation with broadly folded Cryogenian to Terreneuvian strata and unfolded Silurian Numrug complex granite. Fold axes are oriented east-west, broadly parallel with this fault and do not appear to affect Ordovician to Silurian units. Thus, we suggest that this fault and the associated folds in the region are Cambrian in age and that this structure was reactivated sometime during or after the Silurian (Fig. 10). Further northwest, in the Undur-Ulaan Mountain area, this fault zone splays into series of faults in older units, and thus does not provide additional age control (Fig. 2). This fault is broadly aligned with high-angle east-southeast-west-northwest structures that locally have sinistral offset.

An 11-km-long and 5-km-wide ultramafic nappe is present on top of the Khairkhan Formation to the northwest of the Khasagt Khairkhan Range (Fig. 10). This ophiolite fragment likely originated from Khantaishir-Dariv arc and was overthrusted onto the Zavkhan terrane (possibly along fault 3) in the Terreneuvian during the accretion of the Lake terrane (Ruzhentsev and Burashnikov, 1996). This interpretation is supported by the presence of clasts of ultramafic rocks within the mélange of the Khairkhan Formation (Smith et al., 2016).

East-southeast-west-northwest to east-west high-angle faults with sinistral offset are common on the Zavkhan terrane. In the Khukh Davaa region and southwest of Khukh Davaa, these faults are accompanied by a north-northwest-south-southeast conjugate set of normal faults, which define narrow transtensional pull-apart basins that accommodate the Teel Formation (Fig. 2). West of the Khasagt Khairkhan Range and Shivee Tsakhir Mountain a north-northwest-south-southeast fault displaces the early Silurian Numrug complex granite (sample F1128A, Fig. 7E), Taishir Formation carbonates, serpentinized ultramafic rocks, and red beds of the Teel Formation (fault 3, Figures 2 and 10). Displacement on this fault is consistent with down to the east transport with a component of sinistral dip-slip movement. To the east of this fault, folds with east-west-oriented axes in the Khasagt Formation and Tsagaan-Olom Group are truncated. On the western side of this fault, the Terreneuvian thrust fault at the base of the ultramafic rocks and a Cambrian to Ordovician conglomerate unit are truncated (Fig. 10). The northwestern continuation of this fault is stitched by the Permian alkaline granite of the Tonkhil complex exposed in the Ulaantolgoi Gorge that was dated as 286 ± 5 Ma (Kilian et al., 2016). This map relationship constrains movement on this north-northwest-south-southeast fault to between ca. 442 and 286 Ma (Fig. 10), but regionally, the close association of the north-northwest-south-southeast structures and deposition of the Teel Formation in en echelon transtensional pull-apart basins suggests these faults were active during the Late Ordovician to Silurian. It is unclear if the east-southeast-west-northwest to east-west high angle faults were later reactivated.

Relationship to neighboring Proterozoic cratonic fragments of Mongolia

It has been previously assumed that the Proterozoic terranes of Mongolia originated from the same parent craton. While the Zavkhan terrane may have similar Proterozoic basement ages and Neoproterozoic overlap assemblages with the Tuva-Mongolia terranes, our data suggest distinct

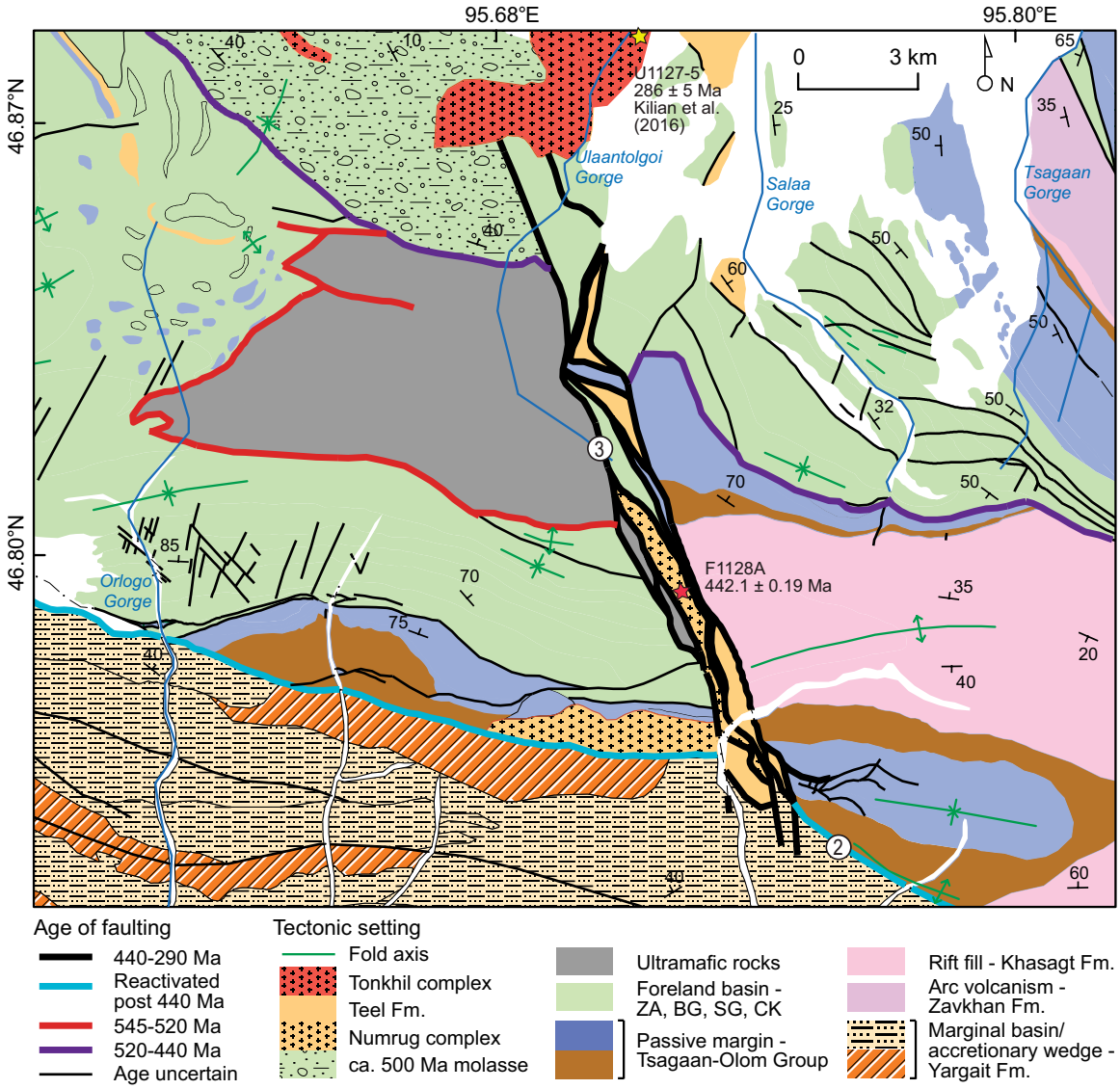

Figure 10. Detailed geologic map of central Zavkhan terrane depicting age of faulting (Fm.—formation). Tectonic setting of the units is described. Description of lithology is outlined in Figures 2 and 4. ZA—Zuun-Arts Formation, BG—Bayangol Formation, SG—Salaagol Formation, and CK—Khairkhan Formation.

differences with the basement ages of the Baidrag terrane and other terranes to the south (Fig. 11).

Crystalline basement of the Tuva-Mongolia terranes (Dergunov, 2001), which include the Sangelin, Hug, Darhad, and Gargan terranes of northern Mongolia (Badarch et al., 2002), was dated in the eastern Sayan Range of Russia with U/Pb TIMS on multigrain bulk zircon fractions between 2163 ± 3 and 1950 ± 10 (Khain et al., 1995). The oldest ophiolitic sequence documented in Mongolia, the Shishkhid ophiolite, is also part of this region and is overlain by a rhyolite flow that was dated with U-Pb SHRIMP on zircon at 800 ± 3 Ma (Kuzmichev et al., 2005). Kuzmichev et al. (2005) interpreted this ophiolite to have formed in a suprasubduction zone setting and to have collided with Tuva-Mongolian continental crust during the late Neoproterozoic. Magmatism related to obduction of Dunzhugar island arc with the Gargan terrane was also dated with U/Pb TIMS on multigrain bulk zircon fractions as 785 ± 11 Ma (Kuzmichev et al., 2001), and active continental margin volcanism of the Sarkhoi Group was dated with U-Pb SHRIMP on zircon at 782 ± 11 Ma (Kuzmichev and Larionov, 2011). The ca. 800–770 Ma Sarkhoi Group can be correlated with the Zavkhan Formation on the Zavkhan terrane (Kuzmichev and Larionov, 2011). Moreover, the overlying Cryogenian glacial diamictites and Neoproterozoic to Cambrian carbonate strata and phosphorite deposits on the Khuvsgul terrane (Fig. 11) can be correlated almost unit for unit with Neoproterozoic strata on the Zavkhan terrane (Macdonald and Jones, 2011). Neoproterozoic to Cambrian strata on the Khuvsgul terrane were also intruded by Epoch 3-Furongian synmetamorphic and postmetamorphic felsic magmatic rocks (Kozakov et al., 1999; Salnikova et al., 2001) and middle to late Paleozoic subalkaline granitic plutons (Badarch et al., 2002).

Basement gneisses of the Baidrag terrane were dated as 2650 ± 30 and 1854 ± 5 Ma (Badarch et al., 2002) and 2364 ± 6, 1839 ± 8, and 1051 ± 10 Ma (Demoux et al., 2009a). It has been suggested that the basement is overlain by Neoproterozoic metasediments (Teraoka et al., 1996), but

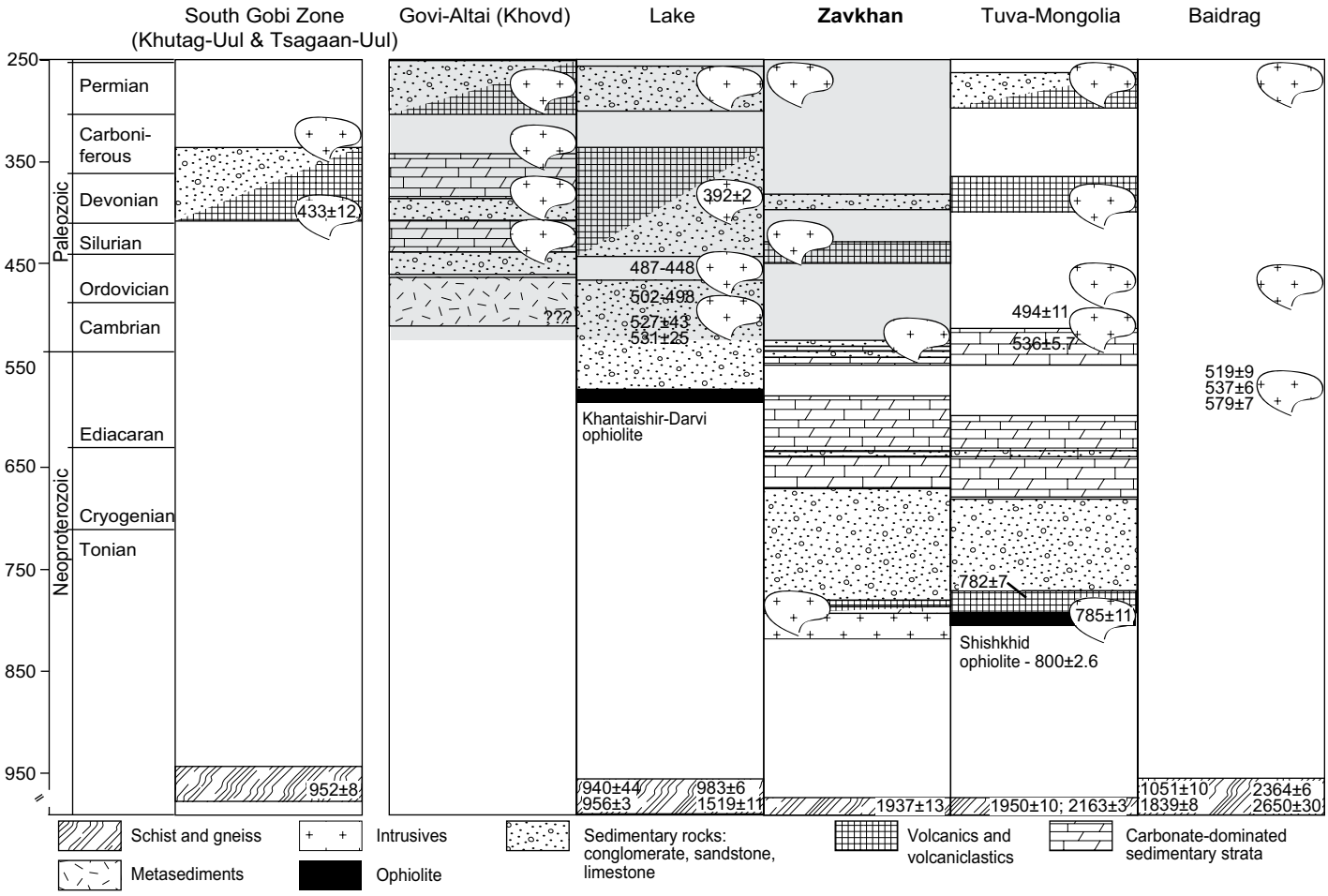

Figure 11. Geology of the neighboring terranes of the Zavkhan terrane in southwestern Mongolia. Basic geologic description is after Badarch et al. (2002). Stratigraphic levels of the samples included in this study are labeled after Figure 2. Recently published magmatic ages are labeled. South Gobi zone (Khutag-Uul and Tsagaan-Uul terranes)-Badarch et al. (2002); Yarmolyuk et al. (2005); Lake terrane-Demoux et al. (2009c); Soejono et al. (2016); Yarmolyuk et al. (2011); Zavkhan terrane–this study; Tuva-Mongolia-Khain et al. (1995); Kuzmichev et al. (2005); Kuzmichev and Larionov (2011); Baidrag-Demoux et al. (2009a).

these are from the Bayankhongor accretionary zone, and no Neoproterozoic overlap assemblage comparable to that on the Zavkhan terrane has been documented. In addition, Demoux et al. (2009a) and Kozakov et al. (2012a) dated magmatism in the northeastern part of the Baidrag terrane at ca. 579–537 Ma that was interpreted to have been related to closure and subduction of the Bayankhongor Ocean to the southwest (Buchan et al., 2001). Metamorphism and magmatism of this age is absent on the Zavkhan terrane.

Further south, near the border with China, the South Gobi zone (Kröner et al., 2010) includes Proterozoic basement of the Tsagaan-Uul and Khutag-Uul terranes (Badarch et al., 2002) and hosts basement gneisses that are dated as 952 ± 8 (Yarmolyuk et al., 2005) and 916 ± 16 Ma (Wang et al., 2001). The gneisses are overlain by Carboniferous and Permian volcano-sedimentary strata and Permian marine sedimentary rocks and are intruded by Carboniferous through lower Cretaceous magmatic rocks (Badarch et al., 2002). Both the basement ages and overlap assemblages have no counterparts in the Zavkhan terrane except for Permian magmatic rocks (Fig. 11). However, the ca. 950 Ma basement ages are similar to those in the Gurvan Bogd Mountains of the Lake terrane (Demoux et al., 2009c).

Detrital zircon provenance of the Zavkhan terrane

Detrital zircon provenance data from Neoproterozoic strata on the Zavkhan terrane were reported in Bold et al. (2016), including data from a quartzite clast from the Zavkhan Formation, cobble conglomerate and sandstones from middle Zavkhan, Maikhan-Uul, and Shuurgat Formations. The comparison did not reveal a perfect match with any of the neighboring terranes such as Siberia, Tarim, North China, and northeast Gondwana (Rojas-Agramonte et al., 2011), which suggested that the detrital population of the Zavkhan terrane is locally derived from the underlying basement and may have its own distinctive late Neoproterozoic characteristics, consistent with the interpretation that the Zavkhan terrane was an independent ribbon continent at this time.

Additional detrital zircon data presented here are from previously undersampled Paleozoic strata in the Zavkhan terrane (Fig. 9). In Figure 12, probability density plots from sedimentary successions on the Zavkhan terrane are compared to data from other terranes; the plots are divided into Precambrian and Paleozoic successions to help reduce bias in interpretation resulting from re-sedimentation. The dominant populations in Precambrian samples (Fig. 12B) are at 2800–2400 Ma (peak of

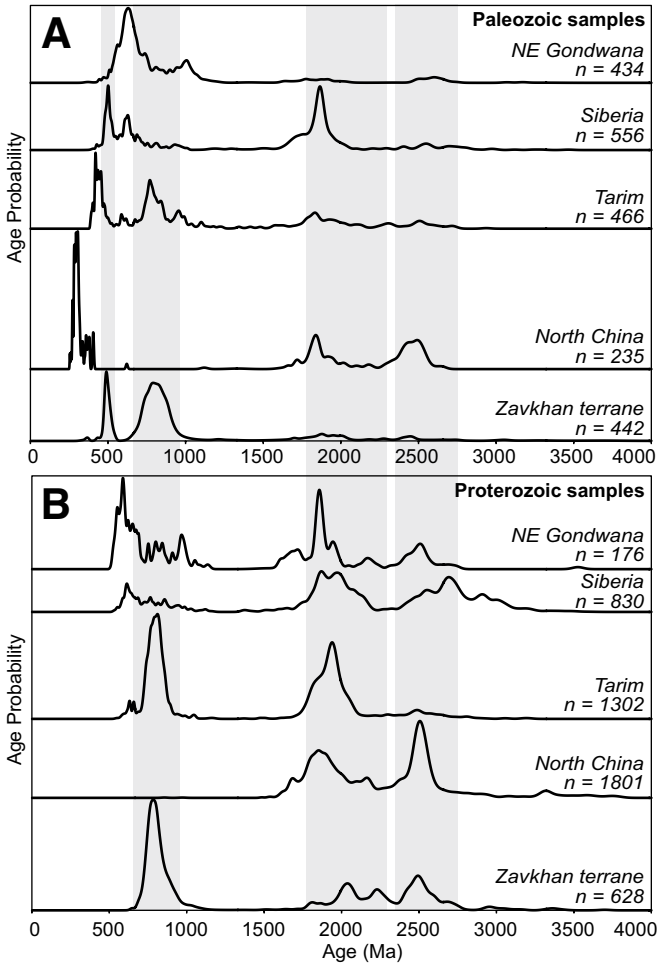

Figure 12. Detrital zircon provenance for the Zavkhan terrane. (A) Normalized probability plots of the Paleozoic samples preserved in northeast Gondwana (Kolodner et al., 2006), Siberia (Gladkochub et al., 2013; Glorie et al., 2014), Tarim (Han et al., 2015), and North China (Li et al., 2009; Yang et al., 2006). (B) Normalized probability plots of the Precambrian successions. The plots were constructed using previous compilations by Rojas-Agramonte et al. (2011) in addition to those of Powerman et al. (2015) and Letnikova et al. (2013) for Siberia, Han et al. (2015) for Tarim, and Xia et al. (2006) for North China.

2500 Ma), 2300–1800 Ma (peak of 2050 Ma), and 900–700 Ma (peak of 800 Ma). An additional population of 550–450 Ma zircon grains (peak of 500 Ma) appears in Paleozoic samples. On the other cratons considered, the 2800–2400 Ma population is present in North China (Rojas-Agramonte et al., 2011; Xia et al., 2006), possibly in Tarim (Han et al., 2015; Rojas-Agramonte et al., 2011; Zhang et al., 2013), and in northeast Gondwana (Rojas-Agramonte et al., 2011). The 2300–1800 Ma population is present in all of the cratons (Letnikova et al., 2013; Powerman et al., 2015; Rojas-Agramonte et al., 2011) except in North China. However, the 900–700 Ma population resembles only that of the Tarim craton, which includes the Aksu blueschist terrane that has been interpreted to have formed along an active continental margin (Zhu et al., 2011). Moreover, the Tarim has ca. 2500 Ma magmatism and ca. 1900 Ma metamorphism age peaks that are also present in the detrital zircon spectra of the Zavkhan terrane (Fig. 12B). Although the basement comparison is not perfect, the best fit for the Zavkhan terrane in the Precambrian appears to be the Tarim craton, which can be tested with additional geochronologic and paleomagnetic studies.

For the Paleozoic comparison, recently published detrital zircon data from North China (Li et al., 2009; Yang et al., 2006), Tarim (Han et al., 2015), southern Siberia (Gladkochub et al., 2013; Glorie et al., 2014), and northeast Gondwana (Kolodner et al., 2006), allow for a more robust comparison (Fig. 12A). A resemblance to the youngest major peak of Mongolia at ca. 500 Ma is present in southern Siberia and is related to the Kalar and Onkolokit granitoids, which intruded through the suture between the Baikal-Muya terrane and Siberia (Powerman et al., 2015) and 520–490 Ma collisional magmatism in the Gorny Altai terrane (Dobretsov et al., 2003). This magmatism and metamorphism may have occurred in response to Ediacaran and Cambrian collision of microcontinents, including collision of the Tuva-Mongolia terranes with the peri-Siberian terranes located near the southern margin of the Siberian craton (Dobretsov and Buslov, 2007). Our detrital zircon data are also consistent with this scenario; however, magmatism and metamorphism of this age is also present in Gondwana associated with the Terra Australis orogeny (Cawood, 2005), and Paleozoic strata from peri-Gondwanan terranes also contain abundant late Ediacaran to late Cambrian detrital zircon(McKenzie et al., 2014; Rojas-Agramonte et al., 2011).

Tectonic model

The newly obtained geochronologic constraints and field observations, including those from the parautochthonous region, have allowed us to propose an updated tectonic model for the Zavkhan terrane. The model spans the Neoproterozoic through early Paleozoic and is supported by map relationships, U-Pb zircon geochronologic constraints (Fig. 11), available whole-rock geochemical data on the magmatic samples (Levashova et al., 2010; Yarmolyuk et al., 2008), and new paleomagnetic constrains (Kilian et al., 2016).

Tonian: Arc Magmatism and Subduction of a Spreading Ridge

Detrital zircon spectra from sedimentary rocks on the Zavkhan terrane lack grains between ca. 1800 and 850 Ma. In the northern portion of the Zavkhan terrane, undeformed granite and gabbroic dikes that may be correlative with the Dund orthocomplex intrude 839 ± 11 Ma gneiss of the Buduun Formation. This relationship suggests that a metamorphic event occurred in the northern portion of the Zavkhan terrane between 839 ± 11 and 811.36 ± 0.24 Ma. Although the nature of this metamorphic event remains enigmatic, based on the zircon chemical compositions (Fig. A21), we suggest it marks the initiation of continental arc volcanism on the Zavkhan terrane.

Mixed volcanic and siliciclastic strata of the Yargait Formation were deposited as a marginal basin fill above the 811.36 ± 0.24 Ma core of the Dund magmatic arc (1 in Fig. 13), either as an intrarc or backarc basin. The Yargait Formation may be correlative with the Oka prism of the Tuva-Mongolia terranes, which has alternatively been interpreted to represent an accretionary wedge related to accretion of the pre-800 ± 3 Ma Shishkhid ophiolite (Kuzmichev et al., 2007). Nonetheless, due to continued subduction to the northeast (in present coordinates), arc-related volcanism persisted to at least ca. 787 Ma (the Zavkhan Formation volcanics, Bold et al., 2016). Alkaline granites dated as 770.31 ± 0.23 Ma (2 in Fig. 13) with geochemistry consistent with an intra-plate setting (Yarmolyuk et al., 2008) are consistent with rifting at the time. In addition, terrestrial sedimentary successions of the Khasagt Formation were deposited between ca. 787 and 717 Ma in narrow, fault-bound basins succeeded by ca. 717–580 Ma rifted passive margin sedimentation of the Tsagaan-Olom Group (Bold et al., 2016). That is, between 787 and 717 Ma, the Zavkhan terrane was transformed from an active continental arc into a ribbon continent with two passive margins. We propose that the

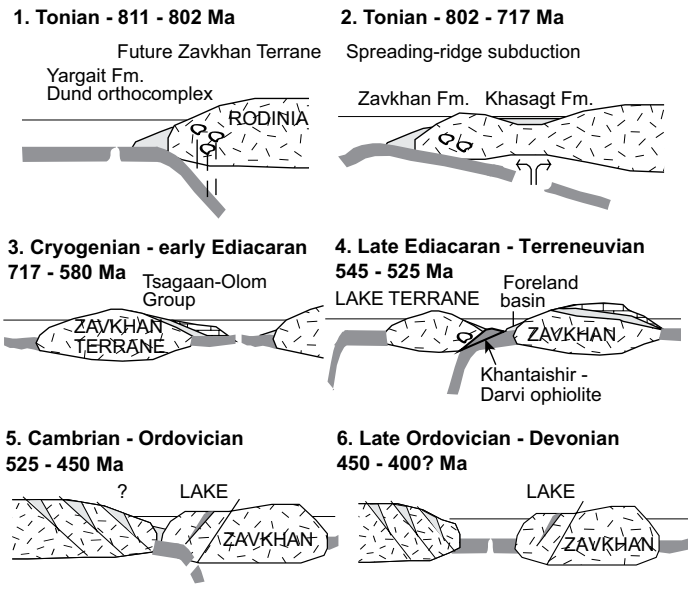

Figure 13. Neoproterozoic to early Paleozoic tectonic model of the Zavkhan terrane. Schematic cross section of the major tectonic events occurred between 811 and 400(?) Ma.

subduction of a spreading ridge (Cole and Stewart, 2009) can explain ophiolite obduction, Neoproterozoic magmatic and stratigraphic patterns, and the development of a ribbon terrane.

Cryogenian to early Ediacaran: Passive margin

Passive margin sedimentation (3 in Fig. 13) of the Tsagaan-Olom Group included deposits from both the Sturtian and Marinoan global Cryogenian glaciations along with their respective cap carbonates in the Cryogenian Maikhan-Uul, Taishir, and Khongor Formations, and the Ediacaran Ol and Shuurgat Formations (Fig. 4; Bold et al., 2016; Macdonald et al., 2009; Rooney et al., 2015). A gap in sedimentation, evidenced by a karsted surface at the top of the Shuurgat Formation that marks an unconformity of ~40 m.y., is inferred from geochemical correlations (Bold et al., 2016; Macdonald et al., 2009). In the neighboring Baidrag terrane (Fig. 1B), ca. 579–537 Ma magmatism and metamorphism (Demoux et al., 2009a) has been associated with the Neoproterozoic closure of the Bayankhongor Ocean (Buchan et al., 2001). Magmatism and metamorphism of this age have not been identified in the Zavkhan terrane, suggesting that the Baidrag and Zavkhan terranes were still separate during the late Ediacaran. Alternatively, the ~40 m.y. late Ediacaran hiatus on the Zavkhan terrane may be the result of the collision between the two. In the hinterland, plagiogranite in suprasubduction zone ophiolites of the Dariv and Khantaishir ranges (Khain et al., 2003) in the Lake terrane were dated as ca. 572 Ma (Khain et al., 2003); however, timing for obduction of this arc is estimated to have occurred by 540–525 Ma (Štípská et al., 2010); this is much later than observed sedimentary hiatus on the Zavkhan terrane, but correlates well with foreland deposition in the Zuun-Arts, Bayangol, Salaagol, and Khairkhan Formations (Macdonald et al., 2009; Smith et al., 2016).

Late Ediacaran to Terreneuvian – Peripheral Pro-Foreland Basin Formation and Obduction of the Lake terrane

The next stage of sedimentation on the Zavkhan terrane is related to late Ediacaran to Terreneuvian foreland basin formation, starting ca. 545 Ma, that accommodated mixed siliciclastic and carbonate strata of the Zuun-Arts, Bayangol, Salaagol, and Khairkhan Formations until ca. 525 Ma (Smith et al., 2016). We propose that these strata were deposited in a peripheral pro-foreland that formed in response to southwest-dipping subduction and flexure of the slab as the Zavkhan terrane collided with the arc and suprasubduction ophiolites of the Lake terrane (4 in Fig. 13). In our model, the pro-foreland basin is suggested to have closed by arc-ophiolite obduction ca. 525 Ma; this is supported by detailed stratigraphic and paleontological constraints (Smith et al., 2016), the youngest detrital zircon date of 533 ± 18 Ma in the siliciclastics of the Bayangol Formation (sample E1105–35.3), granitoid magmatism dated in the Bumbat-Khairkhan area of the Lake terrane at 551–524 Ma (Rudnev et al., 2012), and a ^{40}Ar-^{39}Ar date on a muscovite from eclogite with the accretionary prism of this subduction zone between 548 and 537 Ma (Štípská et al., 2010). This contrasts with earlier models that called for later obduction ca. 470 Ma (Dijkstra et al., 2006; Jian et al., 2014; Kovach et al., 2011; Rudnev et al., 2012; Yarmolyuk et al., 2011).

Cambrian to Late Ordovician – Accretion

After the closure of the foreland basin and arrival of the Lake terrane, 509.56 ± 0.19 and 509.30 ± 0.42 Ma synmetamorphic magmatic rocks with metamorphic rims of 507.07 ± 0.32 Ma were intruded by and post-deformation 496 ± 7 Ma gabbroic dikes and sills. We suggest that the ca. 509–507 Ma magmatism and metamorphism represent an accretionary event that occurred after slab break-off and reversal (5 in Fig. 13). From the perspective of the Mongolian terranes, we refer to this interval as accretionary because orogenesis occurred above a subduction zone on the southern margin of the previously docked Lake terrane; however, it is very possible that this event involved collision with another crustal block. Similar ages of magmatism and metamorphism were reported from the southern margin of Siberia and other peri-Siberian terranes, but also from peri-Gondwanan terranes, and are further supported by our detrital zircon provenance constraints of a major peak at ca. 500 Ma (Fig. 12A) (Dobretsov and Buslov, 2007; Glorie et al., 2014; Rojas-Agramonte et al., 2011).

Late Ordovician to Silurian – Rifting

The bond between the Mongolian terranes and accreted terranes to the south was not strong and did not last long. Late Ordovician to Silurian rift-related magmatism and sedimentation in narrow transtensional grabens are consistent with a major extensional event on the Zavkhan terrane. Moreover, to the south on the Gobi-Altai terrane, a Silurian passive margin sequence developed, consistent with the formation of an open margin and late Paleozoic ocean basin (Kröner et al., 2010; Lehmann et al., 2010).

Yarmolyuk et al. (2011) proposed that 470–440 Ma subalkaline high-Ti basalt, alkaline-ultrabasic complexes, nepheline syenites, alkaline granites, and granosyenites in the Lake terrane are associated with a large igneous province. Alternatively, Soejono et al. (2016) suggested that 459.1 ± 1.8 Ma gabbrodiorites in the western Lake terrane are arc related. We document Late Ordovician to Silurian deposition on the Zavkhan terrane in sinistral transtensional pull-apart basins associated with bimodal volcanism (Kilian et al., 2016), and granite magmatism of the lower Ordovician Numrug complex of the Zavkhan terrane. Kilian et al. (2016) also demonstrate that Late Ordovician volcanics of the Teel Formation of the Zavkhan terrane were emplaced at a subtropical paleolatitude (19° ± 5°). This result is consistent with an association of the Mongolian terranes with an unknown crustal block during Cambrian Epoch 2-Epoch 3 at a latitude consistent with Siberia; however, a late Paleozoic low-latitude overprint suggests subsequent separation given that Siberia continued to travel to north (Cocks and Torsvik, 2007). Complete discussion on available paleomagnetic poles compiled from southwestern Mongolia in association with neighboring stable cratons is in Kilian et al. (2016).

Nevertheless, it is clear that Late Ordovician to Silurian magmatism and deposition on the Lake and Zavkhan terranes was related to extension or transtension, but it remains to be seen if this magmatism was driven by backarc extension or intraplate rifting.

Devonian to Carboniferous – Renewal of Arc Magmatism and Accretionary Tectonics

During the Devonian, a volcanic arc formed on the southern margin of the composite Mongolian terranes (e.g., Badarch et al., 2002; Demoux et al., 2009b; Guy et al., 2015; Kröner et al., 2010; Lamb and Badarch, 1997). The tectonic driver that transformed the Silurian passive margin to a Devonian active margin, referred to as the Tsakhir event, remains unknown (Gibson et al., 2013). Devonian to Carboniferous magmatism and deformation on the Mongolian terranes have been broadly attributed to accretionary processes (e.g., Kröner et al., 2010; Lamb and Badarch, 2001). Late Paleozoic accretion is consistent with the southwestern progression of magmatism: Devonian and Permian magmatic rocks are present in the Lake terrane (e.g., Badarch et al., 2002; Soejono et al., 2016); Carboniferous and Permian magmatic rocks are present in the Gobi-Altai terrane (including the Khovd terrane; Fig. 11) (Kröner et al., 2010; Zacek et al., 2016); and Permian to lower Cretaceous magmatic rocks are present in the South Gobi zone (Badarch et al., 2002).

Comparison with Previous Models, and Paleontological and Paleomagnetic Constraints

As outlined in the Introduction, there are currently three broad classes of models for the Neoproterozoic to Paleozoic tectonic evolution of Mongolia: (1) a peri-Siberian arc model (e.g., Cocks and Torsvik, 2007; Şengör et al., 1993; Tomurtogoo, 2005; Wilhem et al., 2012), (2) an exotic collisional model (e.g., Kröner et al., 2014; Kröner et al., 2010; Mossakovsky et al., 1994; Rojas-Agramonte et al., 2011), and (3) a Siberian accretionary growth model (e.g., Badarch et al., 2002; Windley et al., 2007). The data presented here are most consistent with the exotic collisional model, yet accretionary growth occurred on the composite Mongolian ribbon continent through much of the Paleozoic. Our data suggest that the Proterozoic basement of the Zavkhan terrane is exotic to Siberia and perhaps originated from near the Tarim craton, and that the Zavkhan and other terranes amalgamated and formed the composite Mongolian ribbon continent in the Ediacaran and Terreneuvian. Although many studies link the Mongolian terranes to Siberia based on early Paleozoic paleontological and geological ties (e.g., Kuzmichev and Larionov, 2011; Şengör and Natal'in, 1996; Tomurtogoo, 2005), early Paleozoic stratigraphic, metamorphic, and magmatic belts are truncated by high-angle faults against the Siberian margin. It is possible that the Mongolian ribbon continent collided with Siberia in the Cambrian Epoch 2-Epoch 3, and then rifted away from Siberia in the Late Ordovician before colliding with Siberia again during the Mesozoic (Kilian et al., 2016; Van der Voo et al., 2015); however, it is also possible that the Mongolian ribbon continent was at a latitude similar to Siberia and the Cambrian Epoch 2-Epoch 3 orogenic events in Mongolia and Siberia are merely coincident. Early Paleozoic paleopoles are also consistent with the Zavkhan terrane being near Siberia, but late Paleozoic data suggest the Zavkhan terrane was at a low-latitude when Siberia was at high latitude (Kilian et al., 2016).

Paleontological data are also consistent with an independent Mongolian ribbon continent. Although no trilobites have been described from the Zavkhan terrane, Terreneuvian trilobites from the Khuvsgul terrane (Korobov, 1980; Korobov, 1989) are distinct from Siberian trilobites and those of terranes to the northwest (Álvaro et al., 2013). The presence of Ordovician to Silurian corals and the low diversity Silurian *Tuvaella* brachiopod in Mongolia are consistent with a Furongian to Silurian connection to peri-Siberian terranes (Ulitina et al., 2009); however, although the distinctive *Tuvaella* brachiopod is found throughout southern and northeastern Mongolia and terranes to the northeast, it is not present on the Siberian craton (Wang et al., 2011). Moreover, Ordovician brachiopod assemblages from the Mongolian terranes and Siberia diverge after the Ordovician (Harper et al., 2013). Early and Middle Devonian brachiopods in the Mongolian terranes are different from those occurring in Siberia, North China, and South China (Alekseeva et al., 2001; Blodgett et al., 2002; Hou and Boucot, 1990), and Devonian crinoids in southern Mongolia are most similar to European and North American fauna (Webster and Ariunchimeg, 2004).

Implication for continental growth in the CAOB

Orogenic belts are commonly distinguished as either accretionary or collisional (e.g., Brown et al., 2011; Schulmann and Paterson, 2011). Although the CAOB underwent both accretionary and collisional events, we suggest that distinct tectonic settings were responsible for episodic continental growth and recycling and that the CAOB cannot be lumped into one or another. Accretionary growth occurred around the Mongolian basement terranes during the Ediacaran on the Lake terrane, in the Cambrian on the composite Mongolian ribbon continent, and in the late Paleozoic while they were independent crustal fragments or ribbon continents. These terranes were later trapped and oroclinally duplexed between the Siberian, Tarim, and North China cratons and incorporated into the CAOB. As this region appears to be a prime candidate for future cratonization, we suggest that accretion around continental fragments and ribbon continents and later oroclinal bending and trapping between larger cratons is a viable framework for net continental growth.

CONCLUSIONS

The Zavkhan terrane is one of the Proterozoic cratonic fragments in southwestern Mongolia that make up the core of the CAOB. The Khavchig complex gneiss, which forms the basement of the Zavkhan terrane, was dated as 1967 ± 13 Ma with inherited cores as old as 2469 ± 27 Ma. After a magmatic hiatus of more than 1 b.y., the Zavkhan terrane was intruded by 839 ± 11 Ma granite, which is present as gneiss of the Buduun Formation. Both the Khavchig complex and the Buduun Formation are intruded by 811.36 ± 0.24 Ma arc-related intrusions of Dund orthocomplex that lack a gneissic fabric, suggestive of a Tonian metamorphic event. The Dund orthocomplex is overlain by ca. 811–787 Ma arc-volcanic and volcaniclastic rocks of the Yargait and Zavkhan Formations. The beginning of rifting is marked by alkaline magmatism dated as 770.31 ± 0.23 Ma, and is followed by sedimentation of the Khasagt Formation in narrow rift grabens from 770 to 717 Ma and passive margin sedimentation of the Tsagaan-Olom Group between 717 and 580 Ma. The southern margin of the Zavkhan terrane was reactivated with the obduction of the Lake terrane and the development of a late Ediacaran to Terreneuvian peripheral pro-foreland basin. After this arc-continental fragment collision, Cambrian slab break-off and reversal led to the renewal of magmatism on the Zavkhan terrane, which was by this time embedded in a composite Mongolian ribbon continent. Zircon grains from the Khavchig complex have metamorphic rims dated at 529 ± 22 Ma and are intruded by 509.30 ± 0.42 Ma granite gneiss of the Yesonbulag Formation and 509.56 ± 0.19 Ma unnamed granite, which has a metamorphic zircon rim growth dated as 507.07 ± 0.32 Ma. The succession of ages and a rapid lateral metamorphic gradient are suggestive of Cambrian Epoch 2-Epoch 3 syn-orogenic magmatism. These units are cut by undeformed 496 ± 7 Ma mafic dikes

and sills, providing a tight constraint on the age of Cambrian metamorphism. A Late Ordovician to Silurian rifting event is marked by bimodal magmatism and deposition in narrow pull-apart basins, and by alkaline granite intrusions dated as 442.10 ± 0.19 Ma.

In our proposed tectonic model, we suggest that the Zavkhan terrane traveled alone for much of the Neoproterozoic, possibly collided with an unknown crustal block during Cambrian Epoch 2-Epoch 3 at a latitude consistent with Siberia, but then rifted away during the Ordovician. Much of the continental growth around the Mongolian terranes occurred during the Ediacaran-Terreneuvian, Cambrian, and late Paleozoic, while they were independent crustal fragments or ribbon continents. This is distinct from models of continental growth in the CAOB that invoke direct accretion on the margin of a large craton, and suggests instead that the trapping of crustal fragments and ribbon continents between larger cratons may be an effective mechanism of cratonization.

ACKNOWLEDGMENTS

We thank our field assistants Gerelt Sarantuya, Javzandulam Chuluunbaatar, Munkh-Erdene Delger, Munkh Jugder, Uchral Khuchitbaatar, Otgonbayar Dandar, Ariunsanaa Dorj, Odbayar Erdenebat, Dan Bradley, Tanya Petach and Sarah Moon. We also thank Nicholas Swanson-Hysell and Taylor Kilian for insightful comments and discussions; and the Massachusetts Institute of Technology National Aeronautics and Space Administration Astrobiology Institute node for support.

REFERENCES CITED

Alekseeva, R., Afanasjeva, G., and Shishkina, G., 2001, Lower and Middle Devonian brachiopods of the Far East of Russia and Mongolia: strophomenids and chonetids: Trudy Palaeontological Institute: Russian Academy of Sciences, v. 281, p. 1–132.

Álvaro, J.J., Ahlberg, P., Babcock, L.E., Bordonaro, O.L., Choi, D.K., Cooper, R.A., Ergaliev, G.K., Gapp, I.W., Pour, M.G., and Hughes, N.C., 2013, Global Cambrian trilobite palaeobiogeography assessed using parsimony analysis of endemicity, *in* Harper, D. A. T., and Servais, T., eds., Early Palaeozoic biogeography and palaeogeography: Geological Society of London Memoir 38, p. 273–296, doi:10.1144/M38.19.

Astashkin, V.A., Belyaeva, G., Esakova, N., Osadchaya, D., Pakhomov, N., Pegel, T., Repina, L., Rozanov, A.Y., and Zhuravlev, A.Y., 1995, The Cambrian system of the foldbelts of Russia and Mongolia: correlation chart and explanatory notes: International Union of Geological Sciences Publication, v. 32, p. 132.

Badarch, G., Cunningham, W.D., and Windley, B., 2002, A new terrane subdivision for Mongolia: implications for the Phanerozoic crustal growth of Central Asia: Journal of Asian Earth Sciences, v. 21, p. 87–110, doi:10.1016/S1367-9120(02)00017-2.

Blodgett, R.B., Rohr, D.M., and Boucot, A.J., 2002, Paleozoic links among some Alaskan accreted terranes and Siberia based on megafossils, *in* Miller, E. L., et al., ed., Tectonic Evolution of the Bering Shelf–Chukchi Sea–Arctic Margin and Adjacent Landmasses: Geological Society of America Special Paper 360, p. 273–290, doi:10.1130/0-8137-2360-4.273.

Bold, U., Macdonald, F.A., Smith, E.F., Crowly, J.C., Minjin, C., and Dorjnamjaa, D., 2013, Elevating the Neoproterozoic Tsagaan-Olom Formation to a Group: Mongolian Geoscientist, v. 39, p. 5.

Bold, U., Smith, E.F., Rooney, A.D., Buchwaldt, R., Ramezani, J., Schrag, D.P., and Macdonald, F.A., 2016, Neoproterozoic stratigraphy of the Zavkhan Terrane of Mongolia: The backbone for Cryogenian and Early Ediacaran chemistratigraphic records: American Journal of Science, v. 316, p. 1–63, doi:10.2475/01.2016.01.

Brown, D., et al., 2011, Arc–continent collision: The making of an orogen, *in* Brown, D., and Ryan, P. D., eds., Arc-continent collision: Frontiers in Earth Sciences: Springer, p. 477–493, doi:10.1007/978-3-540-88558-0_17.

Buchan, C., Cunningham, D., Windley, B., and Tomurhuu, D., 2001, Structural and lithological characteristics of the Bayankhongor Ophiolite Zone, Central Mongolia [London]: Journal of the Geological Society, v. 158, p. 445–460, doi:10.1144/jgs.158.3.445.

Bucholz, C.E., Jagoutz, O., Schmidt, M.W., and Sambuu, O., 2014, Phlogopite- and clinopyroxene-dominated fractional crystallization of an alkaline primitive melt: petrology and mineral chemistry of the Dariv Igneous Complex, Western Mongolia: Contributions to Mineralogy and Petrology, v. 167, p. 994, doi:10.1007/s00410-014-0994-6.

Burashnikov, V.V., 1990, Tectonics of the Urgamal zone, early Calidonides of western Mongolia [Phd. thesis]: Russian Academy of Sciences, Moscow, Russia, 25 p.

Cawood, P.A., 2005, Terra Australis Orogen: Rodinia breakup and development of the Pacific and Iapetus margins of Gondwana during the Neoproterozoic and Paleozoic: Earth-Science Reviews, v. 69, p. 249–279, doi:10.1016/j.earscirev.2004.09.001.

Cocks, L., and Torsvik, T.H., 2007, Siberia, the wandering northern terrane, and its changing geography through the Paleozoic: Earth-Science Reviews, v. 82, p. 29–74, doi:10.1016/j.earscirev.2007.02.001.

Cole, R.B., and Stewart, B.W., 2009, Continental margin volcanism at sites of spreading ridge subduction: examples from southern Alaska and western California: Tectonophysics, v. 464, p. 118–136, doi:10.1016/j.tecto.2007.12.005.

Demoux, A., Kroener, A., Badarch, G., Jian, P., Tomurhuu, D., and Wingate, M.T.D., 2009a, Zircon ages from the Baydrag block and the Bayankhongor ophiolite zone: Time constraints on late Neoproterozoic to Cambrian subduction- and accretion-related magmatism in central Mongolia: The Journal of Geology, v. 117, p. 377–397, doi:10.1086/598947.

Demoux, A., Kröner, A., Hegner, E., and Badarch, G., 2009b, Devonian arc-related magmatism in the Tseel terrane of SW Mongolia: chronological and geochemical evidence [London]: Journal of the Geological Society, v. 166, p. 459–471, doi:10.1144/0016-76492008-090.

Demoux, A., Kröner, A., Liu, D., and Badarch, G., 2009c, Precambrian crystalline basement in southern Mongolia as revealed by SHRIMP zircon dating: International Journal of Earth Sciences, v. 98, p. 1365–1380, doi:10.1007/s00531-008-0321-4.

Dergunov, A.B., 2001, Tectonics, Magmatism, and Metallogeny of Mongolia: Hove, U.K., Psychology Press, 288 p.

Dijkstra, A.H., Brouwer, F.M., Cunningham, W.D., Buchan, C., Badarch, G., and Mason, P.R., 2006, Late Neoproterozoic proto-arc ocean crust in the Dariv Range, Western Mongolia: a supra-subduction zone end-member ophiolite [London]: Journal of the Geological Society, v. 163, p. 363–373, doi:10.1144/0016-764904-156.

Dobretsov, N.L., and Buslov, M., 2007, Late Cambrian-Ordovician tectonics and geodynamics of Central Asia: Russian Geology and Geophysics, v. 48, p. 71–82, doi:10.1016/j.rgg.2006.12.006.

Dobretsov, N.L., Buslov, M.M., and Vernikovsky, V.A., 2003, Neoproterozoic to Early Ordovician evolution of the Paleo-Asian Ocean: implications to the break-up of Rodinia: Gondwana Research, v. 6, p. 143–159, doi:10.1016/S1342-937X(05)70966-7.

Evans, D.A.D., Zhuravlev, A.Y., Budney, C.J., and Kirschvink, J.L., 1996, Palaeomagnetism of the Bayan Gol Formation, western Mongolia: Geological Magazine, v. 133, p. 487–496, doi:10.1017/S0016756800007615.

Gibson, T., Myrow, P., Macdonald, F.A., Minjin, C., and Gehrels, G., 2013, Depositional history, tectonics, and detrital zircon geochronology of Ordovician and Devonian strata in southwestern Mongolia: Geological Society of America Bulletin, v. 125, p. 877–893, doi:10.1130/B30746.1.

Gladkochub, D., Stanevich, A., Mazukabzov, A., Donskaya, T., Pisarevsky, S., Nicoll, G., Motova, Z., and Kornilova, T., 2013, Early evolution of the Paleoasian ocean: LA-ICP-MS dating of detrital zircon from Late Precambrian sequences of the southern margin of the Siberian craton: Russian Geology and Geophysics, v. 54, p. 1150–1163, doi:10.1016/j.rgg.2013.09.002.

Glorie, S., De Grave, J., Buslov, M., Zhimulev, F., and Safonova, I.Y., 2014, Detrital zircon provenance of early Palaeozoic sediments at the southwestern margin of the Siberian Craton: Insights from U–Pb geochronology: Journal of Asian Earth Sciences, v. 82, p. 115–123, doi:10.1016/j.jseaes.2013.12.007.

Guy, A., Schulmann, K., Janoušek, V., Štípská, P., Armstrong, R., Belousova, E., Dolgopolova, A., Seltmann, R., Lexa, O., and Jiang, Y., 2015, Geophysical and geochemical nature of relaminated arc-derived lower crust underneath oceanic domain in southern Mongolia: Tectonics, v. 34, p. 1030–1053, doi:10.1002/2015TC003845.

Han, Y., Zhao, G., Sun, M., Eizenhöfer, P.R., Hou, W., Zhang, X., Liu, D., Wang, B., and Zhang, G., 2015, Paleozoic accretionary orogenesis in the Paleo-Asian Ocean: Insights from detrital zircons from Silurian to Carboniferous strata at the northwestern margin of the Tarim Craton: Tectonics, v. 34, p. 334–351, doi:10.1002/2014TC003668.

Harper, D.A., Rasmussen, C.M., Liljeroth, M., Blodgett, R.B., Candela, Y., Jin, J., Percival, I.G., Rong, J.-y., Villas, E., and Zhan, R.-b., 2013, Biodiversity, biogeography and phylogeography of Ordovician rhynchonelliform brachiopods, *in* Harper, D. A. T., and Servais, T., eds., Early Palaeozoic biogeography and palaeogeography: Geological Society of London Memoir 38, p. 127–144, doi:10.1144/M38.11.

Hou, H.F., and Boucot, A.J., 1990, The Balkhash-Mongolia-Okhotsk region of the Old World realm, *in* Mckerrow, W. S., and Scotese, C. R., eds., Palaeozoic palaeogeography and biogeography: Geological Society London Memoir 12, p. 297–303, doi:10.1144/GSL.MEM.1990.012.01.29.

Ilyin, A.V., 1990, Proterozoic supercontinent, its latest Precambrian rifting, breakup, dispersal into smaller continents, and subsidence of their margins: Evidence from Asia: Geology, v. 18, p. 1231–1234, doi:10.1130/0091-7613(1990)018<1231:PSILPR>2.3.CO;2.

Jian, P., Kröner, A., Jahn, B.-m., Windley, B.F., Shi, Y., Zhang, W., Zhang, F., Miao, L., Tomurhuu, D., and Liu, D., 2014, Zircon dating of Neoproterozoic and Cambrian ophiolites in West Mongolia and implications for the timing of orogenic processes in the central part of the Central Asian Orogenic Belt: Earth-Science Reviews, v. 133, p. 62–93, doi:10.1016/j.earscirev.2014.02.006.

Jones, D., 1983, Recognition, Character and Analysis of Tectonostratigraphic Terranes In Western North America: Journal of Geological Education, v. 31, p. 295–303, doi:10.5408/0022-1368-31.4.295.

Khain, E.V., Bibikova, E.V., Kröner, A., Zhuravlev, D.Z., Sklyarov, E.V., Fedotova, A.A., and Kravchenko-Berezhnoy, I.R., 2002, The most ancient ophiolite of the Central Asian fold belt: U–Pb and Pb–Pb zircon ages for the Dunzhugur Complex, Eastern Sayan, Siberia, and geodynamic implications: Earth and Planetary Science Letters, v. 199, p. 311–325, doi:10.1016/S0012-821X(02)00587-3.

Khain, E.V., Bibikova, E.V., Salnikova, E.B., Kroener, A., Gibsher, A.S., Didenko, A.N., Degtyarev, K.E., and Fedotova, A.A., 2003, The palaeo-Asian ocean in the Neoproterozoic and early Palaeozoic: New geochronologic data and palaeotectonic reconstructions: Precambrian Research, v. 122, p. 329–358, doi:10.1016/S0301-9268(02)00218-8.

Khain, E.V., Neymark, L.A., and Amelin, Y.V., 1995, Isotopic-geochronological study of the granites and granite-gneisses of the Gargan block of the eastern Sayan Range in Siberia by Pb-Pb and U-Pb methods on zircons and Sm-Nd method: Doklady Akademii Nauk, v. 342, p. 776–780.

Kilian, T.M., Swanson-Hysell, N.L., Bold, U., Crowley, J., and Macdonald, F.A., 2016, Paleomagnetism of the Teel basalts from the Zavkhan terrane: Implications for Paleozoic paleogeography in Mongolia and the growth of continental crust: Lithosphere, doi:10.1130/L522.1.

Kolodner, K., Avigad, D., McWilliams, M., Wooden, J., Weissbrod, T., and Feinstein, S., 2006, Provenance of north Gondwana Cambrian–Ordovician sandstone: U–Pb SHRIMP dating of detrital zircons from Israel and Jordan: Geological Magazine, v. 143, p. 367–391, doi:10.1017/S0016756805001640.

Korobov, M., 1980, Biostratigrafiya i miomernye trilobity nizhnego kembriya Mongolii [Biostratigraphy and miomerid trilobites from the Lower Cambrian of Mongolia]. The Joint

Soviet-Mongolian Scientific-Research Geological Expedition: The Joint Soviet-Mongolian Scientific-Research Geological Expedition: Transactions, v. 26, p. 5–108.

Korobov, M., 1989, Lower Cambrian biostratigraphy and polymeroid trilobites of Mongolia [in Russian]: Joint Soviet–Mongolian Research Expedition Transactions, v. 48, p. 186–192.

Kovach, V., Yarmolyuk, V., Kovalenko, V., Kozlovskyi, A., Kotov, A., and Terent'eva, L., 2011, Composition, sources, and mechanisms of formation of the continental crust of the Lake Zone of the Central Asian Caledonides. II. Geochemical and Nd isotope data: Petrology, v. 19, p. 399–425, doi:10.1134/S0869591111030064.

Kozakov, I., Kotov, A., Sal'nikova, E., Bibikova, E., Kovach, V., Kirnozova, T., Berezhnaya, N., and Lykhin, D., 1999, Metamorphic age of crystalline complexes of the Tuva-Mongolia Massif: the U-Pb geochronology of granitoids: Petrology, v. 7, p. 177–191.

Kozakov, I., Sal'nikova, E., Yarmolyuk, V., Kozlovsky, A., Kovach, V., Azimov, P.Y., Anisimova, I., Lebedev, V., Enjin, G., and Erdenejargal, C., 2012a, Convergent boundaries and related igneous and metamorphic complexes in Caledonides of Central Asia: Geotectonics, v. 46, p. 16–36, doi:10.1134/S0016852112010037.

Kozakov, I., Yarmolyuk, V., Kovach, V., Bibikova, E., Kirnozova, T., Kozlovskii, A., Plotkina, Y.V., Fugzan, M., Lebedev, V., and Erdenezhargal, C., 2012b, The Early Baikalian crystalline complex in the basement of the Dzabkhan microcontinent of the Early Caledonian orogenic area, Central Asia: Stratigraphy and Geological Correlation, v. 20, p. 231–239, doi: 10.1134/S0869593812030057.

Kravchinsky, V.A., Konstantinov, K.M., and Cogne, J.-P., 2001, Palaeomagnetic study of Vendian and Early Cambrian of South Siberia and Central Mongolia: Was the Siberian platform assembled at this time?: Precambrian Research, v. 110, p. 61–92, doi:10.1016/S0301-9268(01)00181-4.

Kröner, A., Demoux, A., Zack, T., Rojas-Agramonte, Y., Jian, P., Tomurhuu, D., and Barth, M., 2011, Zircon ages for a felsic volcanic rock and arc-related early Palaeozoic sediments on the margin of the Baydrag microcontinent, central Asian orogenic belt, Mongolia: Journal of Asian Earth Sciences, v. 42, p. 1008–1017, doi:10.1016/j.jseaes.2010.09.002.

Kröner, A., Kovach, V., Belousova, E., Hegner, E., Armstrong, R., Dolgopolova, A., Seltmann, R., Alexeiev, D., Hoffmann, J., and Wong, J., 2014, Reassessment of continental growth during the accretionary history of the Central Asian Orogenic Belt: Gondwana Research, v. 25, p. 103–125, doi:10.1016/j.gr.2012.12.023.

Kröner, A., Lehmann, J., Schulmann, K., Demoux, A., Lexa, O., Tomurhuu, D., Štípská, P., Liu, D., and Wingate, M.T., 2010, Lithostratigraphic and geochronological constraints on the evolution of the Central Asian Orogenic Belt in SW Mongolia: Early Paleozoic rifting followed by late Paleozoic accretion: American Journal of Science, v. 310, p. 523–574, doi: 10.2475/07.2010.01.

Kuzmichev, A., Bibikova, E.V., and Zhuravlev, D.Z., 2001, Neoproterozoic (~800 Ma) orogeny in the Tuva-Mongolia Massif (Siberia): island arc-continent collision at the northeast Rodinia margin: Precambrian Research, v. 110, p. 109–126, doi:10.1016/S0301-9268(01)00183-8.

Kuzmichev, A., Kroener, A., Hegner, E., Dunyi, L., and Yusheng, W., 2005, The Shishkhid ophiolite, northern Mongolia: A key to the reconstruction of a Neoproterozoic island-arc system in central Asia: Precambrian Research, v. 138, p. 125–150, doi:10.1016/j.precamres.2005.04.002.

Kuzmichev, A., and Larionov, A., 2011, The Sarkhoi Group in East Sayan: Neoproterozoic (~ 770–800 Ma) volcanic belt of the Andean type: Russian Geology and Geophysics, v. 52, p. 685–700, doi:10.1016/j.rgg.2011.06.001.

Kuzmichev, A., Sklyarov, E., Postnikov, A., and Bibikova, E., 2007, The Oka Belt (Southern Siberia and Northern Mongolia): A Neoproterozoic analog of the Japanese Shimanto Belt?: The Island Arc, v. 16, p. 224–242, doi:10.1111/j.1440-1738.2007.00568.x.

Lamb, M.A., and Badarch, G., 1997, Paleozoic sedimentary basins and volcanic-arc systems of Southern Mongolia: new stratigraphic and sedimentologic constraints: International Geology Review, v. 39, p. 542–576, doi:10.1080/00206819709465288.

Lamb, M.A., and Badarch, G., 2001, Paleozoic sedimentary basins and volcanic arc systems of southern Mongolia: New geochemical and petrographic constraints, *in* Hendrix, M. S., and Davis, G. S., eds., Paleozoic and Mesozoic tectonic evolution of central and eastern Asia: From continental assembly to intracontinental deformation: Geological Society of America Memoir 194, p. 117–149, doi:10.1130/0-8137-1194-0.117.

Lehmann, J., Schulmann, K., Lexa, O., Corsini, M., Kröner, A., Štípská, P., Tomurhuu, D., and Otgonbator, D., 2010, Structural constraints on the evolution of the Central Asian Orogenic Belt in SW Mongolia: American Journal of Science, v. 310, p. 575–628, doi:10.2475/07.2010.02.

Letnikova, E., Kuznetsov, A., Vishnevskaya, I., Veshcheva, S., Proshenkin, A., and Geng, H., 2013, The Vendian passive continental margin in the southern Siberian Craton: Geochemical and isotopic (Sr, Sm–Nd) evidence and U–Pb dating of detrital zircons by the LA-ICP-MS method: Russian Geology and Geophysics, v. 54, p. 1177–1194, doi:10.1016/j.rgg.2013.09.004.

Levashova, N.M., Kalugin, V.M., Gibsher, A.S., Yff, J., Ryabinin, A.B., Meert, J., and Malone, S.J., 2010, The origin of the Baydaric microcontinent, Mongolia: Constraints from paleomagnetism and geochronology: Tectonophysics, v. 485, p. 306–320, doi:10.1016/j.tecto.2010.01.012.

Li, H., Xu, Y., Huang, X., He, B., Luo, Z., and Yan, B., 2009, Activation of northern margin of the North China Craton in Late Paleozoic: Evidence from U-Pb dating and Hf isotopes of detrital zircons from the Upper Carboniferous Taiyuan Formation in the Ningwu-Jingle basin: Chinese Science Bulletin, v. 54, p. 677–686, doi:10.1007/s11434-008-0444-9.

Ludwig, K.R., 2008, User's manual for Isoplot 3.70: A geochronological Toolkit for Microsoft Excel, Berkeley Geochronology Center Special Publication 4.

Macdonald, F. A., and Jones, D. S., 2011, The Khubsugul Group, northern Mongolia, *in* E., A., Halverson, G. P., and Shields, G., eds., The geological record of Neoproterozoic glaciations: Geological Society of London 36.1, p. 339–345, doi:10.1144/M36.30.

Macdonald, F.A., Jones, D.S., and Schrag, D.P., 2009, Stratigraphic and tectonic implications of a new glacial diamictite-cap carbonate couplet in southwestern Mongolia: Geology, v. 37, p. 123–126, doi:10.1130/G24797A.1.

Macdonald, F.A., Ryan-Davis, J., Coish, R., Crowley, J., and Karabinos, P., 2014, A newly identified Gondwanan terrane in the northern Appalachian Mountains: Implications for the Taconic orogeny and closure of the Iapetus Ocean: Geology, v. 42, p. 539–542, doi: 10.1130/G35659.1.

Macdonald, F.A., Schmitz, M.D., Crowley, J.L., Roots, C.F., Jones, D.S., Maloof, A.C., Strauss, J.V., Cohen, P.A., Johnston, D.T., and Schrag, D.P., 2010, Calibrating the Cryogenian: Science, v. 327, p. 1241–1243, doi:10.1126/science.1183325.

McKenzie, N.R., Hughes, N.C., Gill, B.C., and Myrow, P.M., 2014, Plate tectonic influences on Neoproterozoic–early Paleozoic climate and animal evolution: Geology, v. 42, p. 127–130, doi:10.1130/G34962.1.

Mossakovsky, A., Ruzhentsev, S., Samygin, S., and Kheraskova, T., 1994, Central Asian fold belt: geodynamic evolution and formation history: Geotectonics, v. 27, p. 445–474.

Petrosyan, N., 1967, Stratigraphic importance of the Devonian flora of the USSR, *in* Oswald, D.H., ed., International Symposium on the Devonian System: Volume 2: Canadian Society of Petroleum Geologists, p. 579–586.

Pojeta, J., Jr., 1986, Devonian rocks and Lower and Middle Devonian pelecypods of Guangxi, China, and the Traverse Group of Michigan: U.S. Geological Survey Professional Paper 1394A-G, p. 106.

Powerman, V., Shatsillo, A., Chumakov, N., Kapitonov, I., and Hourigan, J., 2015, Interaction between the Central Asian Orogenic Belt (CAOB) and the Siberian craton as recorded by detrital zircon suites from Transbaikalia: Precambrian Research, v. 267, p. 39–71, doi: 10.1016/j.precamres.2015.05.015.

Rizza, M., Ritz, J.F., Prentice, C., Vassallo, R., Braucher, R., Larroque, C., Arzhannikova, A., Arzhannikov, S., Mahan, S., and Massault, M., 2015, Earthquake Geology of the Bulnay Fault (Mongolia): Bulletin of the Seismological Society of America, v. 105, p. 72–93, doi: 10.1785/0120140119.

Rojas-Agramonte, Y., Kröner, A., Demoux, A., Xia, X., Wang, W., Donskaya, T., Liu, D., and Sun, M., 2011, Detrital and xenocrystic zircon ages from Neoproterozoic to Palaeozoic arc terranes of Mongolia: significance for the origin of crustal fragments in the Central Asian Orogenic Belt: Gondwana Research, v. 19, p. 751–763, doi:10.1016/j.gr.2010.10.004.

Rooney, A.D., Strauss, J.V., Brandon, A.D., and Macdonald, F.A., 2015, A Cryogenian chronology: Two long-lasting synchronous Neoproterozoic glaciations: Geology, v. 43, p. 459–462, doi:10.1130/G36511.1.

Rudnev, S., Izokh, A., Borisenko, A., Shelepaev, R., Orihashi, Y., Lobanov, K., and Vishnevsky, A., 2012, Early Paleozoic magmatism in the Bumbat-Hairhan area of the Lake Zone in western Mongolia (geological, petrochemical, and geochronological data): Russian Geology and Geophysics, v. 53, p. 425–441, doi:10.1016/j.rgg.2012.03.004.

Ruzhentsev, S.V., and Burashnikov, V.V., 1996, Tectonics of the western Mongolian Salairides: Geotectonics, v. 29, p. 379–394.

Salnikova, E., Kozakov, I., Kotov, A., Kröner, A., Todt, W., Bibikova, E., Nutman, A., Yakovleva, S., and Kovach, V., 2001, Age of Palaeozoic granites and metamorphism in the Tuvino-Mongolian Massif of the Central Asian Mobile Belt: loss of a Precambrian microcontinent: Precambrian Research, v. 110, p. 143–164, doi:10.1016/S0301-9268(01)00185-1.

Samozvantsen, B.A., Tsukerik, A.B., and Golyakov, B.I., 1981, Results of 1: 200 000 scale geological mapping and general prospecting in Great Lakes depression of western branches of Hangay Highland: Geologic Information Center Open-File Report 3576, Total pages, 1036.

Schulmann, K., and Paterson, S., 2011, Geodynamics: Asian continental growth: Nature Geoscience, v. 4, p. 827–829, doi:10.1038/ngeo1339.

Şengör, A., Natal'In, B., and Burtman, V., 1993, Evolution of the Altaid tectonic collage and Palaeozoic crustal growth in Eurasia: Nature, v. 364, p. 299–307, doi:10.1038/364299a0.

Şengör, A.C., and Natal'in, B.A., 1996, Paleotectonics of Asia: fragments of synthesis, *in* Yin, A., and Harrison, M., eds., The Tectonic Evolution of Asia: Cambridge, Cambridge University Press, p. 486–640.

Sláma, J., Košler, J., Condon, D.J., Crowley, J.L., Gerdes, A., Hanchar, J.M., Horstwood, M.S., Morris, G.A., Nasdala, L., and Norberg, N., 2008, Plešovice zircon—a new natural reference material for U–Pb and Hf isotopic microanalysis: Chemical Geology, v. 249, p. 1–35, doi:10.1016/j.chemgeo.2007.11.005.

Smith, E.F., Macdonald, F.A., Petach, T.A., Bold, U., and Schrag, D.P., 2016, Integrated stratigraphic, geochemical, and paleontological late Ediacaran to early Cambrian records from southwestern Mongolia: Geological Society of America Bulletin, v. 128, p. 442–468, doi:10.1130/B31248.1.

Soejono, I., Buriánek, D., Svojtka, M., Zacek, V., Cap, P., and Janousek, V., 2016, Mid-Ordovician and Late Devonian magmatism in the Togtokhinshil Complex: new insight into the formation and accretionary evolution of the Lake Zone (western Mongolia): Journal of Geosciences (Prague), v. 61, p. 5–23, doi:10.3190/jgeosci.208.

Štípská, P., Schulmann, K., Lehmann, J., Corsini, M., Lexa, O., and Tomurhuu, D., 2010, Early Cambrian eclogites in SW Mongolia: evidence that the Palaeo-Asian Ocean suture extends further east than expected: Journal of Metamorphic Geology, v. 28, p. 915–933, doi: 10.1111/j.1525-1314.2010.00899.x.

Teraoka, Y., Suzuki, M., Tungalag, F., Ichinnorov, N., and Sakamari, Y., 1996, Tectonic framework of the Bayankhongor area, west Mongolia: Bulletin of the Geological Survey of Japan, v. 47, p. 447–455.

Togtokh, D., Baatarkhuyag, A., and Bayardalai, S., 1995, Results of 1:200000 scale geological mapping and general prospecting: Geological Information Center Open-File Report 4861, Total pages, 1575.

Tomurtogoo, O., 2005, Tectonics and structural evolution of Mongolia, *in* Seltmann, R., et al., eds., Geodynamics and Metallogeny of Mongolia With a Special Emphasis on Copper and Gold Deposits: International Association on the Genesis of Ore Deposits (IAGOD) Guidebook Series, Volume 11, p. 5–12.

Ulitina, L., Bondarenko, O., and Minjin, C., 2009, Evolution of the taxonomic diversity of Mongolian Ordovician-Silurian corals: Paleontological Journal, v. 43, p. 499–505, doi: 10.1134/S0031030109050049.

Van der Voo, R., van Hinsbergen, D.J., Domeier, M., Spakman, W., and Torsvik, T.H., 2015, Latest Jurassic–earliest Cretaceous closure of the Mongol-Okhotsk Ocean: A paleomagnetic and seismological-tomographic analysis, *in* Anderson, T. H., et al., ed., Late Jurassic margin of Laurasia–A record of faulting accommodating plate rotation: Geological Society of America Special Papers 513, p. 589–606, doi:10.1130/2015.2513(19).

Wang, C., Li, N., Sun, Y., and Zong, P., 2011, Distribution of Tuvaella brachiopod fauna and its tectonic significance: Journal of Earth Science, v. 22, p. 11–19, doi:10.1007/s12583-011-0153-1.

Wang, T., Zheng, Y., Gehrels, G., and Mu, Z., 2001, Geochronological evidence for existence of South Mongolian microcontinent—A zircon U-Pb age of granitoid gneisses from the Yagan-Onch Hayrhan metamorphic core complex: Chinese Science Bulletin, v. 46, p. 2005–2008, doi:10.1007/BF02901917.

Webster, G.D., and Ariunchimeg, Y., 2004, The northern most Emsian crinoids known, a Devonian fauna from the Chuluun Formation, Shine Jinst area, Southern Mongolia: Geobios, v. 37, p. 481–487, doi:10.1016/j.geobios.2003.07.001.

Wilhem, C., Windley, B.F., and Stampfli, G.M., 2012, The Altaids of Central Asia: A tectonic and evolutionary innovative review: Earth-Science Reviews, v. 113, p. 303–341, doi:10.1016/j.earscirev.2012.04.001.

Windley, B.F., Alexeiev, D., Xiao, W., Kroener, A., and Badarch, G., 2007, Tectonic models for accretion of the Central Asian Orogenic Belt: Journal of the Geological Society, v. 164, p. 31–47, doi:10.1144/0016-76492006-022.

Xia, X., Sun, M., Zhao, G., and Luo, Y., 2006, LA-ICP-MS U–Pb geochronology of detrital zircons from the Jining Complex, North China Craton and its tectonic significance: Precambrian Research, v. 144, p. 199–212, doi:10.1016/j.precamres.2005.11.004.

Xiao, W., Windley, B.F., Hao, J., and Zhai, M., 2003, Accretion leading to collision and the Permian Solonker suture, Inner Mongolia, China: termination of the central Asian orogenic belt: Tectonics, v. 22, doi:10.1029/2002TC001484.

Yakubchuk, A., 2004, Architecture and mineral deposit settings of the Altaid orogenic collage: a revised model: Journal of Asian Earth Sciences, v. 23, p. 761–779, doi:10.1016/j.jseaes.2004.01.006.

Yang, J.-H., Wu, F.-Y., Shao, J.-A., Wilde, S.A., Xie, L.-W., and Liu, X.-M., 2006, Constraints on the timing of uplift of the Yanshan Fold and Thrust Belt, North China: Earth and Planetary Science Letters, v. 246, p. 336–352, doi:10.1016/j.epsl.2006.04.029.

Yang, J., Cawood, P.A., Du, Y., Huang, H., Huang, H., and Tao, P., 2012, Large Igneous Province and magmatic arc sourced Permian–Triassic volcanogenic sediments in China: Sedimentary Geology, v. 261, p. 120–131, doi:10.1016/j.sedgeo.2012.03.018.

Yarmolyuk, V., Kovach, V., Kovalenko, V., Salnikova, E., Kozlovskii, A., Kotov, A., Yakovleva, S., and Fedoseenko, A., 2011, Composition, sources, and mechanism of continental crust growth in the Lake Zone of the Central Asian Caledonides: I. Geological and geochronological data: Petrology, v. 19, p. 55–78, doi:10.1134/S0869591111010085.

Yarmolyuk, V., Kovalenko, V., Anisimova, I., Sal'nikova, E., Kovach, V., Kozakov, I., Kozlovsky, A., Kudryashova, E., Kotov, A., and Plotkina, Y.V., 2008, Late Riphean alkali granites of the Zabhan microcontinent: evidence for the timing of Rodinia breakup and formation of microcontinents in the Central Asian Fold Belt: Doklady Earth Sciences, v. 420, p. 583–588, doi:10.1134/S1028334X08040132.

Yarmolyuk, V., Kovalenko, V., Sal'nikova, E., Kozakov, I., Kotov, A., Kovach, V., Vladykin, N., and Yakovleva, S., 2005, U-Pb-Age of syn-and postmetamorphic granitoids from Southern Mongolia-evidence for the presence of Grenvillides in the Central Asian Fold Belt: Doklady Earth Sciences, v. 404, p. 986–990.

Zacek, V., Burianek, D., Pecskay, Z., and Skoda, R., 2016, Astrophyllite-alkali amphibole rhyolite, an evidence of early Permian A-type alkaline volcanism in the western Mongolian Altai: Journal of Geosciences (Prague), v. 61, p. 93–103.

Zhang, C.-L., Zou, H.-B., Li, H.-K., and Wang, H.-Y., 2013, Tectonic framework and evolution of the Tarim Block in NW China: Gondwana Research, v. 23, p. 1306–1315, doi:10.1016/j.gr.2012.05.009.

Zhao, Y., Song, B., and Zhang, S.H., 2006, The Central Mongolian microcontinent: Its Yangtze affinity and tectonic implications, *in* Proceedings Symposium on continental growth and orogeny in Asia, Taipei, Taiwan, p. 135–136.

Zhu, W., Zheng, B., Shu, L., Ma, D., Wu, H., Li, Y., Huang, W., and Yu, J., 2011, Neoproterozoic tectonic evolution of the Precambrian Aksu blueschist terrane, northwestern Tarim, China: insights from LA-ICP-MS zircon U–Pb ages and geochemical data: Precambrian Research, v. 185, p. 215–230, doi:10.1016/j.precamres.2011.01.012.

MANUSCRIPT RECEIVED 4 APRIL 2016
REVISED MANUSCRIPT RECEIVED 30 JULY 2016
MANUSCRIPT ACCEPTED 6 OCTOBER 2016

Printed in the USA